Autry, R.J., Paugh, S.W., Carter, R. et al. I*ntegrative genomic analyses reveal mechanisms of glucocorticoid resistance in acute lymphoblastic leukemia*. **Nat Cancer** 1, 329–344 (2020). This version of the article has been accepted for publication, after peer review (when applicable) and is subject to Springer Nature's AM terms of use, but is not the Version of Record and does not reflect post-acceptance improvements, or any corrections. The Version of Record is available online at: https://doi.org/10.1038/s43018-020-0037-3

Integrative genomic analyses reveal mechanisms of glucocorticoid resistance in acute lymphoblastic leukemia

Robert J. Autry[1,2,3], **Steven W. Paugh**[1,2], **Robert Carter**[4,5], **Lei Shi**[6], **Jingjing Liu**[5], **Daniel C. Ferguson**[1,2], **Calvin E. Lau**[1,2,7], **Erik J. Bonten**[1,2], **Wenjian Yang**[1,2], **J. Robert McCorkle**[1,2], **Jordan A. Beard**[1,2], **John C. Panetta**[2], **Jonathan D. Diedrich**[1,2], **Kristine R. Crews**[1,2], **Deqing Pei**[6], **Christopher J. Coke**[1,2], **Sivaraman Natarajan**[4,5], **Alireza Khatamian**[5], **Seth E. Karol**[1,4,8], **Elixabet Lopez-Lopez**[1,2], **Barthelemy Diouf**[1,2], **Colton Smith**[1,2], **Yoshihiro Gocho**[1,2], **Kohei Hagiwara**[5], **Kathryn G. Roberts**[1,9], **Stanley Pounds**[6], **Steven M. Kornblau**[10], **Wendy Stock**[11], **Elisabeth M. Paietta**[12], **Mark R. Litzow**[13], **Hiroto Inaba**[1,4], **Charles G. Mullighan**[1,4,9], **Sima Jeha**[1,4,9], **Ching-Hon Pui**[1,4,9], **Cheng Cheng**[6], **Daniel Savic**[1,2], **Jiyang Yu**[5], **Charles Gawad**[4,5], **Mary V. Relling**[1,2,3], **Jun J. Yang**[1,2,4], **William E. Evans**[1,2,3,*]

[1]Hematological Malignancies Program and Center for Precision Medicine in Leukemia, St. Jude Children's Research Hospital, Memphis, TN 38105, USA

[2]Department of Pharmaceutical Sciences, St. Jude Children's Research Hospital, Memphis, Tennessee, USA

[3]Integrated Biomedical Sciences Program, University of Tennessee Health Science Center, Memphis, Tennessee, USA

[4]Department of Oncology, St. Jude Children's Research Hospital, Memphis, Tennessee, USA

[5]Department of Computational Biology, St. Jude Children's Research Hospital, Memphis, Tennessee, USA

[6]Department of Biostatistics, St. Jude Children's Research Hospital, Memphis, Tennessee, USA

[7]Pediatric Oncology Education Program, St. Jude Children's Research Hospital, Memphis Tennessee, USA

[8]Comprehensive Cancer Center, St. Jude Children's Research Hospital, Memphis, Tennessee, USA

[9]Department of Pathology, St. Jude Children's Research Hospital, Memphis, Tennessee, USA

[10]Department of Leukemia, Division of Cancer Medicine, The University of Texas MD Anderson Cancer Center, Houston, Texas, USA

[11]Hematopoiesis and Hematological Malignancies Program, University of Chicago, Chicago, Illinois, USA

[12]Department of Medicine, Albert Einstein College of Medicine, Montefiore Medical Center, North Division, Bronx, New York, USA

[13]Division of Hematology and Department of Internal Medicine, Mayo Clinic., Rochester, Minnesota, USA

Abstract

Identification of genomic and epigenomic determinants of drug resistance provides important insights for improving cancer treatment. Using agnostic genome-wide interrogation of mRNA and miRNA expression, DNA methylation, SNPs, CNAs and SNVs/Indels in primary human acute lymphoblastic leukemia cells, we identified 463 genomic features associated with glucocorticoid resistance. Gene-level aggregation identified 118 overlapping genes, 15 of which were confirmed by genome-wide CRISPR screen. Collectively, this identified 30 of 38 (79%) known glucocorticoid-resistance genes/miRNAs and all 38 known resistance pathways, while revealing 14 genes not previously associated with glucocorticoid-resistance. Single cell RNAseq and network-based transcriptomic modelling corroborated the top previously undiscovered gene, CELSR2. Manipulation of CELSR2 recapitulated glucocorticoid resistance in human leukemia cell lines and revealed a synergistic drug combination (prednisolone and venetoclax) that mitigated resistance in mouse xenograft models. These findings illustrate the power of an integrative genomic strategy for elucidating genes and pathways conferring drug resistance in cancer cells.

Drug resistance is a major cause of treatment failure for disseminated human cancers. [1] Acute lymphoblastic leukemia (ALL) has long served as a model for developing curative chemotherapy for disseminated malignancies. Long-term disease-free survival in childhood ALL has increased dramatically in recent decades, with 5-year event-free survival approaching 90%, yet drug resistance makes it less curable in adult patients and it remains a leading cause of cancer deaths in children [2]. Much of the improvement in cure rates can be ascribed to refinement of therapy based on improved understanding of clinical and biological characteristics of the disease and the intensification of treatment when there is poor early response or persistence of minimal residual disease (MRD) [2–5]. Glucocorticoids, such as prednisone (PRED) and dexamethasone (DEX), are essential components of curative combination chemotherapy for ALL in adults and children [6] and the intrinsic sensitivity of ALL cells to glucocorticoids, as measured *ex vivo,* is predictive of treatment outcome (event-free survival or survival) in childhood ALL [1,7–9]. Although several mechanisms of leukemia cell resistance to glucocorticoids have been identified [10–13], the genomic and epigenetic determinants of *de novo* glucocorticoid resistance remain poorly understood. Whole genome sequencing offers a comprehensive approach for identifying sequence variants that confer drug resistance, but this technology does not assess the complex interaction of multiple genomic, transcriptomic and epigenetic mechanisms.[14] In the current study, we integrated genome-wide interrogation of multiple genomic and epigenetic features of primary leukemia cells to identify genes associated with drug resistance, using glucocorticoids as a model. This directly identified over 78% of genes and 100% of pathways previously associated with glucocorticoid resistance and further revealed 14 genes

not previously known to confer glucocorticoid resistance. Collectively, this represents an agnostic, multi-dimensional genome-wide strategy for discovery of genomic mechanisms of drug resistance in primary cancer cells.

Results

Drug sensitivity and treatment response

The sensitivity to prednisolone of primary leukemia cells from bone marrow aspirates of 225 newly diagnosed patients with B-lineage ALL ranged over 5 orders of magnitude (LC_{50} 0.00176 −1387.4μM) (Figure. 1a). Using previously reported criteria, patients with prednisolone LC_{50} values <0.1 μM were classified as sensitive, those >64 μM were classified as resistant, and the remaining patients were designated as intermediate sensitivity. [15]. Patients whose leukemia cells were intermediate or resistant to prednisolone were significantly more likely to have minimal residual disease (MRD) >1% at day 15–19 of remission induction therapy ($p=1.3 \times 10^{-5}$; Figure 1b.). Likewise, MRD at the end of remission induction therapy, on day 46 of St. Jude Total XV protocol (TOTXV) or day 42 of St. Jude Total XVI protocol (TOTXVI), was more likely to be >0.1% in patients whose leukemia cells were intermediate or resistant to prednisolone ($p=1.1 \times 10^{-4}$; Figure 1b.). These MRD levels have been previously associated with a significantly worse event free survival.[16–18]

Polygenomics of glucocorticoid resistance

Six distinct genomic/epigenetic features were interrogated genome-wide in primary leukemia cells and assessed for their association with prednisolone resistance (LC_{50}) in two independent patient cohorts [Extended Data Fig. 1]. Hierarchical clustering of each feature type was performed to identify genomic features (mRNA, miRNA, CpG methylation, single nucleotide polymorphisms [SNPs], copy number alterations [CNAs] and SNV/Indels [WES]) that best discriminated prednisolone sensitive and resistant ALL (Supplementary Table 1). These analyses identified 254 mRNA expression probes (permutation p-value < 8.2×10^{-5}), 203 CpG methylation sites (permutation p-value < 1×10^{-5}), 49 miRNA probes (permutation p-value < 1×10^{-5}), 380 SNPs (permutation p-value< 1×10^{-5}), 25 CNA segments (permutation p-value < 4.5×10^{-4}) and 227 WES mutations (permutation p-value < 1×10^{-5}) that best individually discriminated prednisolone resistant from prednisolone sensitive ALL (Figure 2.; Extended Data Fig. 2 a–b; Supplementary Table 1). This mRNA expression signature was verified in two independent validation cohorts (Extended Data Fig. 2c–d). Collectively, these features identified 192 distinct genes associated with prednisolone resistance.

Connectivity of these genomic features (miRNA, methylation, SNPs, CNAs and SNV/Indels) was initially assessed based on significant relation to mRNA expression and filtered based on biologically relevant criteria (*cis* CpG site or miRNA binding site as described in *Methods*), revealing that the expression of 94% of the significant mRNAs was significantly associated with at least one of the other genomic features and five were connected to all other features (*IDI1,ITPR3, PTPRF, WNK1, and PAX5*; Supplementary Table 2). mRNA expression probes that were associated with LC_{50} in the polygenomic analysis were also

associated with treatment response, as assessed by the *in vivo* level of residual leukemia on day 15–19 and day 42–46 of remission induction treatment (Extended Data Fig. 2e). Prednisolone LC_{50} across all subtypes revealed some ALL subtypes that were more resistant than others, but prednisolone resistant and sensitive cases were documented in all major subtypes (Extended Data Fig. 2f.)

Genes identified in the polygenomic analysis (Figure 2.) were interrogated for relevant pathway connections (Supplementary Table 3.), that included B-cell development (*PAX5* mRNA, *FLT3* methylation and SNV/Indel, *ITGA4 SNP eQTL*), B-cell receptor signaling (e.g., *CD19* methylation, *PAX5* mRNA, *TCF3* mRNA), non-canonical Wnt signaling (*CELSR1/2* methylation and mRNA, *ROR1* mRNA), IL7R-signaling (e.g., *IL2RG* mRNA, *JAK3 SNP eQTL*), SWI/SNF complex (*SMARCA4* mRNA*),* TGF-B signaling, apoptosis signaling (*BCL2* methylation, *FAS* mRNA), drug transporters (*ABCC1* methylation), and inflammatory signaling (*CASP1* methylation and mRNA, *NLRP3* methylation).

Gene level integration of multiple genomic variants

To assess the influence of each gene on prednisolone resistance, we aggregated p-values of all genomic features within 50 kilobases upstream or downstream of the coding region for all annotated human genes (n = 19,725), to obtain a gene-level TAP (Truncated Aggregation of P-values) statistic with its associated p-value (see *Methods*). This identified 903 genes associated with prednisolone resistance ($p<5.38\times10^{-4}$; Figure 3a; Supplementary Table 4). Extended Data Fig. 3a–d illustrate four gene-level plots and their TAP statistic. *SMARCA4 and NLRP3* illustrate genes previously associated with prednisolone resistance, [15,19] whereas *CELSR2 and PTTG1IP* illustrate the top two candidate genes in current study (Extended Data Fig. 3a–d Supplementary Table 5). Many of these genes, 118/463 (25%), are common between the gene-level TAP analysis and the polygenomic analysis that assessed each feature independently (Figure 3c). Pathway analysis of genes significant in the TAP analysis is detailed in Supplementary Table 3.

Validation by genome-wide CRISPR knockout screen

To validate hits by an orthogonal method, we performed genome-wide CRISPR/Cas9 knockout screening using the GeCKOv2 library [20]. In cells treated with 100uM prednisolone, we identified 1024 genes that were significantly “knockout enriched” in prednisolone resistant leukemia cells (FDR < 5.2×10^{-7}; Figure 3b, Supplementary Table 6). *NR3C1*, the gene encoding the GR, was the top “knockout enriched” gene ($p= 4.6\times10^{-78}$). This screen identified genes affecting multiple cellular functions, including several pro-apoptotic genes (*BAK1, PMAIP, APAF1, CAPN3/10*) and genes involved in GR signaling, cell-cell communication genes (*ITGA5/B1,CELSR2*), modulators of GR transcriptional activation (*NRIP1, JUN),* inhibitors of NF-kB kinase (*IKBKB, IKBKG*), B-cell developmental genes (*BCL6*), glucocorticoid biosynthetic components (*HSD3B1/7, CYP11B1*), cytokine signaling genes (e.g.,*IL4R, IL1RAPL2*), toll-like receptor signaling (*TLR6, IRAK3, TNF),* inhibitors of PI3K signaling genes (*PTEN),* and other genes previously associated with glucocorticoid resistance (*TBL1XR1 and CNR2).* When the knockout enriched genes were used to perform clustering on the RNA-seq from a 320

patient validation cohort, this significantly discriminated resistant and sensitive leukemias (clustering p- value = 0.006).

We also identified 1000 genes that were significantly "knockout reduced" (i.e. depletion of gRNAs targeted to knockout these genes, FDR < 1.19×10^{-14}; Supplementary Table 6), suggesting their absence enhanced glucocorticoid sensitivity. This revealed genes associated with various signaling pathways such as inflammasome activation (*NLRP3, NLRC3, CARD11/17),* NF-kB signaling (*NFKB2, NFKIB2*), JNK/SAPK signaling (e.g., *MAPK9[*JNK2*], RAC2), PI3K* signaling *(PI3KR1/3, PI3KR3, PRKCB),* apoptotic proteins (*FAS),* TNF signaling and growth factor signaling (*FGFR2, FGF10*) [Supplementary Table 3]. The knockout reduced genes were also able to discriminate glucocorticoid resistant and sensitive leukemias in the 320 patient validation cohort (clustering p-value = 1.7×10^{-5}).

Genes significant by multiple methods

As summarized in Figure 3c, 247 genes were significant by at least two methods and significantly discriminated resistance in the 320 patient validation cohort (clustering p-value = 0.001), as did the 118 genes significant by both TAP and polygenomic analyses (clustering p-value = 1.34×10^{-6}), and the 50 genes in both CRISPR and the polygenomic analysis (clustering p-value = 6×10^{-4}). Fifteen genes (*CELSR2*, *MAPK13*, *PARD3*, *CALN1*, *DAP*, *RBMS2*, *PTTG1IP*, *NLRP3*, *FAM13A*, *TAOK3*, *DCLRE1A*, *RASGRF2*, *FBXO9*, *GALNT1* and *TMEM126A*) were significant by all three methods, thereby constituting the top candidate genes (Figure 3c; Supplementary Table 5), and they discriminated sensitive from resistant leukemias in the validation cohort (clustering p-value = 1×10^{-4}). Only one of the 15 top candidate genes (*NLRP3*) has been previously associated with glucocorticoid resistance [15]. The statistical likelihood of a gene being significant by all three methods by chance is very low (p = 8.2×10^{-79}; Supplementary Notes).

Corroboration of known resistance mechanisms

To assess the robustness of our approach, we compared genes/miRNAs that were significantly related to glucocorticoid resistance in our analyses, to genes involved in previously published mechanisms of glucocorticoid resistance (35 genes and three miRNAs, identified as described in *Methods*, summarized in Supplementary Table 7). Of these 38 previously reported genes/miRNAs, 30 (79%) were found to be significant by one or more of our three methods. This improved to 38/38 (100%) genes/miRNA when we included other members of the involved resistance pathway using StringDB (strict criteria as defined in *Methods*).

CELSR2 knockdown alters transcriptional response and prednisolone resistance

CELSR2 was the top candidate gene by all three methods, with decreased expression associated with glucocorticoid resistance in the discovery cohort (p= 3.3×10^{-10}; Figure 3d.; Supplementary Table 5). *CELSR2* remained significant after adjusting for leukemia molecular subtype (p < 9.5×10^{-6}). Lower *CELSR2* expression in glucocorticoid resistant ALL was subsequently validated in primary leukemia cells from two independent validation cohorts, one comprising 320 pediatric and adult patients with newly diagnosed ALL (p= 8.3×10^{-8}; Figure 3e), and the other comprising 145 pediatric patients with newly diagnosed

ALL (p= 0.033). We also documented in primary leukemia cells that patients with low expression of *CELSR2* (defined as mRNA ≤ the lowest quartile of expression) had significantly lower expression of the GR (*NR3C1*; p-value = 1.7×10^{-4}; Figure 3f, g). We also observed 5 patients with copy number alterations in *CELSR2*, and 4 were resistant to glucocorticoids. Only two patients had predicted damaging missense mutations in *CELSR2*, one was prednisolone resistant and the other prednisolone intermediate sensitivity. Reduction of *CELSR2* expression in two human ALL cell lines by shRNA (Figure 3h), significantly increased prednisolone resistance (LC_{50}) compared to non-targeting control (Figure 3i). There was a 12.7-fold increase in LC_{50} in *CELSR2* knockdown NALM-6 cells (0.026 ± 0.033μM vs 0.37 ± 0.1 μM (mean ± s.e.m), $p=7.8\times10^{-5}$), and a 20-fold increase in LC_{50} in 697 cells (0.095±0.003 μM vs. 1.98±0.046 μM (mean ± s.e.m), $p=9.0\times10^{-4}$).

To assess the mechanism of GC resistance, we identified differentially expressed genes and alterations in global transcriptional effects of glucocorticoids in *CELSR2* knockdown cells. Knockdown of *CELSR2* led to a significant decrease in basal expression of the GR (*NR3C1)* in both NALM-6 cells (1.8-fold decrease; $p= 1.34\times10^{-7}$ Figure 4a), and 697 cells (1.3 fold-decrease, $p= 4.3\times10^{-5}$; [Extended Data Fig. 4a]). Decreased expression of total cellular GR in *CELSR2* knockdown cell lines was more prominent after 24 hours of prednisolone treatment in the NALM-6 cell line (2.3-fold decrease; $p = 2.8\times10^{-12}$: Figure 4b;), and in the 697 cell line (1.44 fold-decrease, $p= 1.45\times10^{-5}$; [Extended Data Fig. 4b]). A second shRNA was used to confirm on-target specificity and phenotype (Extended Data Fig. 4c.). Stable *CELSR2* protein knockdown (Extended Data Fig 4e.) showed decreased glucocorticoid receptor protein expression (Extended Data Fig. 4f) in ALL cells. Stable re-expression of GR (97% of control) significantly re-sensitized leukemia cells to prednisolone (Figure 4c–d; two-tailed t-test p-value = 0.02).

After activation of the GR with 24 hours of glucocorticoid treatment, many genes were differentially expressed in *CELSR2* knockdown versus control ALL cells, including a robust upregulation of the antiapoptotic gene *BCL2* in *CELSR2* knockdown cells, documented at the transcriptional (2.5-fold increase; $p= 3.7\times10^{-12}$; Figure 4b) and protein level (1.3-fold increase; p = 0.0128; Extended Data Fig. 4g), consistent with the known repressive effect of activated GR on *BCL2* [21]. *BCL2L11* (Bim), a pro-apoptotic gene known to be up-regulated by glucocorticoids [22] did not exhibit upregulation in *CELSR2* knockdown cells after 24 hours of prednisolone treatment (1.3-fold decrease, compared to a 1.8-fold increase in non-targeting control $p= 4.6\times10^{-6}$; Extended Data Fig. 4g), yielding a lower ratio of BIM/BCL2 protein expression in the *CELSR2* knockdown NALM-6 cells after 24 hours of prednisolone treatment. (Extended Data Fig. 4h). Genome-wide analysis of glucocorticoid-induced gene expression changes in NALM-6 cells (3 replicate experiments) identified 415 genes that were induced at least three-fold compared to untreated cells, 72% (298/415) of which had lower induction (at least 25% less induction) by prednisolone treatment in *CELSR2* knockdown cells, consistent with lower GR (Figure 4e). Furthermore, 69 genes were repressed by at least three-fold in control cells, and 90% (62/69) had at least 25% lower repression in *CELSR2* knockdown cells (Figure 4e; Supplementary Table 8). Similar results were observed in the 697 cell line (Extended Data Fig. 4i.).

Mitigation of glucocorticoid resistance caused by low *CELSR2* expression via inhibition of *BCL2*

Because the anti-apoptotic gene *BCL-2* was highly induced in CELSR2 knockdown cells after prednisolone treatment, we tested venetoclax (a *BCL-2* inhibitor) for its ability to mitigate glucocorticoid resistance in ALL cells with low *CELSR2* expression. When *CELSR2* knockdown ALL cells were treated for 72 hours with prednisolone (0.954nM - 4mM) and varying concentrations of venetoclax, synergy was evident in two human leukemia cell lines (NALM-6 α =2.07; 697 α =2.47; Figure 5a.; Extended Data Fig. 5a,c), but synergy was greatly increased in leukemia cells in which *CELSR2* was knocked down (NALM-6 α = 5.22; 697 α = 4.38; Figure 5b; Extended Data Fig. 5b,d), and confirmed using other methods for assessing drug synergy (Loewe's additivity and ZIP method; data not shown).

In mice inoculated with NALM-6 leukemia cells with shRNA targeting *CELSR2*, there was a significant prolongation of survival in mice treated with venetoclax 50 mg/kg plus dexamethasone, compared to dexamethasone alone (median survival 60 vs 69 days; p=0.0062; Figure 5d) or venetoclax alone (median survival 56 vs 69 days; p=0.0046; Figure 5d). In mice inoculated with NALM-6 leukemia cells with the non-targeting control shRNA (NTC), there was modest but significant prolongation of survival when treated with venetoclax 100 mg/kg plus dexamethasone compared to dexamethasone alone (median survival 39 vs 41 days; p=0.02; Figure 5c), whereas there was not significant improvement with the lower dosage of venetoclax (50 mg/kg) combined with dexamethasone (p=0.836; Figure 5c), consistent with greater synergy in ALL with lower CELSR2 expression.

To verify these findings in primary leukemia cells, we documented that primary leukemia cells (n= 96 patients) that were resistant to prednisolone were significantly more sensitive to venetoclax (p=0.014; Extended Data Fig. 5e.). As reported for other malignancies [23,24], higher BCL-2 expression in primary ALL cells was associated with increased sensitivity to venetoclax ($p=2.5\times10^{-3}$; Extended Data Fig. 5f.).

We also measured the effects of the two drugs given separately or together in primary leukemia cells isolated from the bone marrow or peripheral blood of six patients (3 freshly isolated and 3 xenograft samples). In the two prednisolone sensitive patients, we observed low levels of additivity/synergy, whereas in the four leukemias that were intermediate or resistant to prednisolone, we documented greater synergy based on significantly higher alpha values in all cases (Extended Data Fig. 5g). Three of the four prednisolone resistant patients exhibited much lower mRNA expression of *CELSR2* and *NR3C1* when compared to the prednisolone sensitive patients (Extended Data Fig. 5h), and primary ALL cells from all four of the prednisolone resistant patients exhibited decreased ability to induce the pro-apoptotic protein *BIM* when treated with 10μM prednisolone for 24 hours (data not shown).

CELSR2 is a negative hub driver of prednisolone resistance

We used NetBID[25], a data-driven systems biology approach, to reconstruct a B-ALL-specific interactome (B-ALLi),composed of "hubs" representing central components of larger regulatory networks, using RNA-seq profiles of 185 B-ALL patients in the

TARGET[26] cohort (Figure 6a). B-ALLi identified hub drivers whose network activities differed significantly in prednisolone resistant versus sensitive leukemia cells from two patient cohorts (SJCRH TOTXV and TOTXVI; Figure 6b). Known glucocorticoid resistance genes including *SMARCA4*, *PAX5*, *CASP1* were significantly enriched in NetBID top predictions (p=0.011, Extended Data Fig. 6a). Network topology analysis of the top 48 NetBID drivers ($p<5 \times 10^{-5}$, Figure 6b, Extended Data Fig. 6b) identified *CELSR2* as a hub that modulated other top drivers (Figure 6c). NetBID-inferred activity of *CELSR2* was markedly down-regulated ($p=8.6 \times 10^{-8}$, Figure 6d) in prednisolone resistant relative to sensitive leukemias, as was the expression of *CELSR2* (Figure 6b). More strikingly, *CELSR2* regulons (Extended Data Fig. 6c) inferred by NetBID from baseline RNA-Seq profiles of B-ALL patients were significantly enriched among differentially expressed genes in ALL cells after *CELSR2* knockdown ($p=1 \times 10^{-4}$ in NALM-6 and $p=1 \times 10^{-3}$ in 697 cells, Figure 6e, Extended Data Fig. 6d). Several previously reported glucocorticoid resistance genes (e.g. *TSC22D3, IL1B* and *TP53INP1),* were also regulated by *CELSR2* ($p=1.8 \times 10^{-3}$ in NALM-6 and p=0.01 in 697, Extended Data Fig. 6e).

CELSR2 expression is significantly related to PAX5

NetBID analysis also identified *CELSR2* as a top downstream target of *PAX5* (Extended Data Fig. 7a.). For *CELSR2,* the most highly co-expressed gene in primary ALL cells was *PAX5,* which was highly positively correlated in leukemia cells from 203 patients ($p= 3\times10^{-11}$; Extended Data Fig. 7b). Accordingly, lower expression of *PAX5* was observed in leukemia cells with higher prednisolone LC_{50} ($p = 7.47\times10^{-05}$; Supplementary Table 1.). Recent studies have highlighted the importance of chromatin accessibility in the discovery of regulators of glucocorticoid resistance.[27,28] ATAC-seq profiles of multiple human leukemia cell lines revealed open chromatin regions in proximity to the *CELSR2* coding region. When combined with ENCODE transcription factor binding site data,[29] *PAX5* binding sites were found within the cis-regulatory elements of *CELSR2* in the B-lymphocyte cell line GM12878 (Extended Data Fig. 7c). Furthermore, CHIP-seq peaks for *PAX5* in NALM-6 ALL cells confirmed that *PAX5* binds in these open chromatin regions in a leukemia cell line (Extended Data Fig. 7c). We constructed a multivariate model using the expression of all miRNAs associated with *CELSR2* as co-variates along with PAX5 mRNA, revealing that *PAX5* expression accounted for about 25% of the variability in *CELSR2* expression ($p= 1.6\times10^{-12}$), and mir-31–5p accounted for an additional 4% of the variability in *CELSR2* expression (p=0.002). Alone, miR-31–5p was significantly negatively associated with *CELSR2* expression (p= 0.001), as was *PAX5* ($p=3\times10^{-11}$). PAX5 knockdown in NALM-6 cells (Extended Data Fig. 7d) showed significant reduction in both *CELSR2* (two-tailed t-test p-value =0.0003; Extended Data Fig. 7e) and *NR3C1* (two-tailed t-test p-value<0.0001; Extended Data Fig. 7f).

scRNA-seq reveals clonality of resistance genes

We performed single cell RNA-seq on primary ALL cells from a patient with prednisolone sensitive leukemia (LC_{50} = 0.091μM) and from a patient with prednisolone resistant leukemia (LC_{50} = 1006μM). Primary leukemia cells from each patient were treated *ex vivo* with 63μM prednisolone or incubated in media without prednisolone, and single-cell RNA sequencing was used to generate clusters of surviving cells after 96 hours, based on their

gene expression profiles. As expected, the prednisolone sensitive leukemia had a pronounced reduction in CD19+ cells (Figure 7a, d; Extended Data Fig. 8a–c; $p < 2\times10^{-16}$), whereas the resistant leukemia retained a high percentage of CD19+ cells after prednisolone treatment (Figure 7a; Extended Data Fig. 8d–f; Supplementary Table 9). Single-cell RNA sequencing documented that the sensitive leukemia had higher *CELSR2* expression before treatment than the resistant leukemia, which had essentially undetectable *de novo* expression of *CELSR2* (Figure 7b; FDR = 0.009). BCL-2 expression was significantly higher in the resistant patient after prednisolone treatment compared to control, and greater than in the sensitive leukemia (Figure 7c, f; FDR = 0.005; Supplementary Table 9).

CELSR2 is a mediator of non-canonical Wnt signaling

To assess the potential effects of CELSR2 on GR expression, we performed ATAC-seq to interrogate regulatory regions upstream of the *NR3C1* gene in three glucocorticoid sensitive and three glucocorticoid resistant ALL cell lines, revealing enriched open chromatin for the GR in the sensitive cell lines compared to resistant ALL cells, in regions overlapping H3K27-acetylation peaks from ENCODE (Extended Data Fig. 9a–d). The REH cell line has a known stop gain mutation in *NR3C1*, which leads to glucocorticoid resistance independent of *CELSR2*. ENCODE transcription factor binding data revealed binding sites for *TEAD4 (Hippo signaling), NFATC1* and the AP-1 components cJun and fos within the upstream regulatory regions of *NR3C1* (Extended Data Fig. 9d).

Because CELSR2 is known to regulate non-canonical WNT signaling [30], we quantitated the expression of NFAT, pJNK, cJun, phos-cJun and *NR3C1* in *CELSR2* knockdown cells and control cells (Figure 8 and Extended Data Fig. 9 e–h). This documented significantly lower nuclear expression of phosphorylated JNK (p=0.015) and lower phosphorylation of its target cJun at serine 63 (p=0.0017), which was also evident in cells treated with prednisolone (24hr at 10μM; p=0.03). We also documented decreased nuclear GR levels in *CELSR2* knockdown compared to control cells in both treated (p=0.03) and untreated (p=0.005) cells. Cytoplasmic levels of the GR were also significantly lower in *CELSR2* knockdown cells compared to controls, in both prednisolone treated (p=0.03) and untreated (p=0.0002) cells (Extended Data Fig. 9 g–h).

Discussion

Although there are several known genetic and epigenetic mechanisms of glucocorticoid resistance in ALL, many leukemias are resistant for reasons that have remained unknown. To assess the potential of agnostic genome-wide interrogation of multiple forms of genomic and epigenetic variants to identify mechanisms of drug resistance in human cancer, we assessed *de novo* prednisolone resistance in primary ALL cells from newly diagnosed patients. The *ex vivo* sensitivity of ALL cells to glucocorticoids is related to treatment outcome in ALL [1,9], and was related to the persistence of residual leukemia (MRD) in our patient cohort. We identified 655 inter-related genomic features associated with 463 genes and 48 miRNAs that discriminated prednisolone sensitive and resistant ALL based on somatic variation in mRNA, miRNA, CpG methylation, SNPs, CNAs or SNVs/Indels. Notably, 94% of the mRNAs discriminating glucocorticoid sensitive and resistant ALL were statistically

associated with one or more of the significant miRNA, cis CpG-methylation sites, SNPs, CNAs or SNVs/Indels within coding regions, indicating the interconnectivity of these genomic features. To assess the increased utility of interrogating multiple data types simultaneously, we performed multivariable analysis using a forward selection method to generate a best fit model using all feature types, yielding a model that explained ~47% of the variability in prednisolone LC_{50} (93% before bias correction). This model contained 32 features: 2 mRNAs (*CELSR2* and *FAM13A)* both of which are in our top 15 genes, 12 methylation probes (including *BCL2*), 2 miRNAs and 14 SNPs (Supplementary Table 1), supporting the use of multiple data types together in genomic studies of complex phenotypes (e.g., drug resistance). Furthermore, many features not included in the multivariable model were significantly related to other features in the model, providing enhanced confidence in the genes identified. Gene-level integration of these six genomic features identified 118 genes that were significantly associated with prednisolone resistance by both the polygenomic and the TAP methods. Fifteen of these genes were also significant in a genome-wide CRISPR-knockout screen, 14 of which have not been previously associated with glucocorticoid resistance. The statistical probability of capturing 15 genes in all three analyses by chance is extremely small ($p= 8.2\times10^{-79}$; see Supplementary Notes).

To assess the robustness of our approach, we compared genes identified in the current analyses with genes previously associated with glucocorticoid resistance in ALL[15,19,31–58]. This revealed that 30 of 38 (79%) genes previously shown to confer glucocorticoid resistance in ALL were directly identified by our agnostic, integrative polygenomic strategy. Some previously described genes such as *CREBBP* were not found directly, but genes known to be associated with their function (*CREB1*) were found. When we included genes in the same biological pathway, our method captured all 38 pathways previously shown to confer glucocorticoid resistance in ALL. Re-discovery of this large number of known mechanisms of resistance gives confidence that many of the previously unknown mechanisms are likely genuine, either as independent mechanisms or as members of common pathways.

CELSR2 was the top gene downregulated in glucocorticoid resistant ALL and decreasing *CELSR2* expression recapitulated glucocorticoid resistance in human leukemia cell lines. This also revealed genes that exhibited significantly altered expression as a consequence of reducing *CELSR2* expression, including markedly lower expression of the GR and higher expression of anti-apoptotic *BCL2* following prednisolone treatment. We showed that co-administration of a BCL2 inhibitor (venetoclax) mitigated glucocorticoid resistance due to low *CELSR2* expression, documenting greater synergy in ALL cell lines in which *CELSR2* had been knocked down and in primary leukemia cells with low *CELSR2* expression. Low *CELSR2* expression was documented in approximately half of glucocorticoid resistant ALL patients (48%), suggesting that co-treatment with venetoclax could impact a large number of patients and this combination may have even broader utility since other mechanisms of glucocorticoid resistance involve lower GR expression or function[15]. We also observed a significant increase in survival *in vivo* in mice inoculated with *CELSR2* knockdown ALL cells when venetoclax (50 mg/kg) was given in combination with glucocorticoids (Figure 5c–d), consistent with our *ex vivo* findings of greater venetoclax sensitivity in primary leukemia cells and human ALL cells lines with low *CELSR2* expression (Figure 5a–b).

NetBID network analyses using interactome data generated in the independent TARGET [26] cohort, corroborated many of the genes and pathways that we found significant, including *CELSR2*. This is consistent with *CELSR2* and its network of interacting genes acting as a master regulatory network influencing the sensitivity of leukemia cells to prednisolone.

CELSR2 is a membrane-bound G-protein coupled receptor that alters gene expression via non-canonical WNT signaling [30] and HIPPO signaling [59], and is involved in cell-cell interactions. Manipulation of *CELSR2* in ALL cells led to alterations in downstream non-canonical Wnt targets, increasing the expression of NFAT1 and cJun and decreasing the phosphorylation of cJun at the total protein level [60], consistent with the documented decreased activation of JNK via phosphorylation at Thr 183/Tyr 185. Increasing the level of cJun represses transcription of the GR[61], as we observed in primary ALL cells with low *CELSR2* expression. We further documented significantly lower nuclear levels of phosphorylated JNK and phosphorylated cJun, which forms a heterodimer with *FOS* (AP1) to drive expression of *NR3C1* (GR), consistent with lower *NR3C1* expression we observed in ALL with low *CELSR2* expression.

Taken together, we have shown that integration of agnostic multi-dimensional somatic genome variants can identify discrete mechanisms of drug resistance in primary leukemia cells, reliably rediscovering known mechanisms of resistance and revealing mechanisms not previously reported. Our findings indicate that interrogating multiple types of genomic variation improves the ability to discover mechanisms of resistance, compared to interrogating only one type of genome variation. Applying this strategy, we discovered a previously undescribed mechanism involving low expression of *CELSR2* in approximately 50% of glucocorticoid resistant ALL patients, causing lower expression of GR and overexpression of *BCL2*, which can be mitigated by co-treatment with the BCL2-inhibitor venetoclax. These findings represent a broad strategy for discovering genetic and epigenetic mechanisms by which cancer cells develop resistance to chemotherapy, and for revealing therapeutic strategies to mitigate resistance.

Methods

Patients

The sensitivity of primary leukemia cells to prednisolone was determined *ex vivo* for a total of 444 patients aged 18 years or younger with newly diagnosed ALL. Of these, 298 patients were enrolled in the St. Jude Total Therapy XV (TOTXV, NCT00137111) or XVI (TOTXVI, NCT00549848) protocol, the initial 225 were the “discovery” cohort and the subsequent 73 constituted a validation cohort. We also used publicly available mRNA expression data and prednisolone LC_{50} values for 145 European pediatric ALL patients previously described in detail[62] as a second validation cohort. Also, 45 T-lineage leukemia patients from St. Jude Total Therapy XV or XVI protocols were included for investigating ALL subtype differences in prednisolone sensitivity. Leukemia cells from an additional cohort of 335 patients with ALL were studied: 226 pediatric patients (14 St. Jude Total Therapy XV, 182 St. Jude Total Therapy XVI [73 from validation cohort] and 30 from St. Jude Total Therapy XVII) and 109 adult patients (66 from the Eastern Cooperative Oncology Group, 33 from M.D. Anderson Cancer Center, 8 from the University of Chicago and 2 from the Alliance for

Clinical Trials in Oncology) were included to further assess the expression of *CELSR2*; in a subset of these patients (n=96) the sensitivity to venetoclax was measured. The level of minimal residual disease (MRD) in bone marrow was determined by flow cytometry and/or polymerase chain reaction at day 15–19 and after completion of induction, as previously described.[63] Written informed consent was obtained from all patients or their parents or guardians. The use of these samples was approved by the institutional review board at St. Jude Children's Research Hospital.

Mice

Unconditioned mice were seven to nine weeks old when injected with leukemia. Daily observations were carried out on the mice and they were sacrificed when leukemia cells reached 50% in the peripheral blood, or the veterinarian determined they showed clinical symptoms (ruffled fur, respiratory stress, hindlimb paralysis, or significantly decreased mobility).This study was performed in accordance with the recommendations in the Guide for the Care and Use of Laboratory Animals of the National Institutes of Health. Mice were maintained in an American Association of Laboratory Animal Care accredited facility and were treated using a protocol approved by the St. Jude Animal Care and Use Committee (Protocol Number: 580–100498) in accordance with NIH guidelines. NOD. Cg-Prkdc scid Il2rg tm1Wjl/SzJ (NSG) mice were obtained from the St. Jude colony for all experiments and were kept under pathogen free conditions. Animals were sacrificed by carbon dioxide asphyxiation using the gradual displacement method, consistent with the American Veterinary Medical Association Guidelines for the Euthanasia of Animals: 2013 Edition. Great efforts were made to minimize suffering.

Human Leukemia Cell lines

Human B-lineage acute lymphoblastic leukemia cell lines (NALM-6 and 697) were maintained in RPMI 1640 supplemented with 10% fetal bovine serum (FBS) and 2mM L-glutamine at 37° C with 5% CO_2. *CELSR2* knockdown cell lines were generated in NALM-6 and 697 cells transduced with lentivirus containing short-hairpin RNA targeting *CELSR2* (MISSION pLKO.1-puro shRNA TRCN0000011243; sequence : 5'-CCGGGCCACTGAAGACACTGACATACTCGAGTATGTCAGTGTCTTCAGTGGCTTTTT or TRCN0000011240 sequence: 5'-CCGGCGCTTGGACAAAGGGAACTTTCTCGAGAAAGTTCCCTTTGTCCAAGCGTTTTT; Sigma-Aldrich) or a non-targeting control (MISSION pLKO.1-puro Non-mammalian shRNA control (SHC002); Sigma-Aldrich), and selected in media containing 5μg/mL puromycin. *PAX5* knockdown NALM-6 cell lines were generated by transducing with lentivirus short-hairpin RNA targeting *PAX5* (MISSION pLKO.1-puro shRNA TRCN0000016059; sequence: 5'-CCGGCCCTCAGTATTCCTCGTACAACTCGAGTTGTACGAGGAATACTGAGGGTTTTT; Sigma-Aldrich) or a non-targeting control (MISSION pLKO.1-puro Non-mammalian shRNA control (SHC002); Sigma-Aldrich), and selected in media containing 5μg/mL puromycin.

GR rescue experiments were performed by stable lentiviral transduction of non-target control or shRNA targeting *CELSR2* transduced NALM-6 cells with plx304 vector

(Addgene) with cDNA of GR (Origene; RC220189) tagged with V5 or GFP control. These cells were then selected with 15μg/mL Blasticidin and 5μg/mL Puromycin and assessed for *in vitro* prednisolone sensitivity at 72hr.

To constitutively express Cas9 in the NALM-6 cell line, we transduced cells with lentivirus containing the Cas9 expression vector (Addgene: 52962) and selected cells in media containing 15μg/ml blasticidin (Sigma-Aldrich).

Prednisolone *ex vivo* resistance assay

Primary leukemia cells were isolated from the bone marrow or peripheral blood of newly diagnosed ALL patients, and tested for prednisolone sensitivity by MTT assay, as previously described [15,62]. In brief, cells were seeded in a 96-well plate at a concentration of 2×10^6 cells/mL for primary cells, in phenol red-free RPMI 1640 medium supplemented with 20% FBS, 2 mM L-glutamine, 100 IU/mL penicillin, 100 μg/mL streptomycin, 0.25 μg/mL Amphotericin B, and 1X insulin-transferrin-selenium supplement or 2.0×10^5 cells/mL for ALL cell lines, in phenol red-free RPMI 1640 with 10% FBS and 2mM L-glutamine. In wells of round-bottom 96-well plates, 80 μL of each cell suspension was combined with 20 μL of methylprednisolone at varying concentrations (Solu-Medrol®, Pfizer) diluted serially. Plates were incubated at 37° C in 5% CO_2 for a total of 96 hours (primary ALL) or 72 hours (ALL cell lines).10 μL of 5 mg/mL MTT (3-(4,5-dimethyl-2-thiazolyl)-2,5-diphenyl-tetrazolium bromide) was added to each well for the final 6 hours of incubation. Acidified isopropanol was used to solubilize formazan crystals and absorbance was measured at 562 nm with a background correction of 720 nm, (uQuant, BioTek Instruments). For ALL cell lines, the CellTiterGlo® Assay (Promega) was used to measure prednisolone LC_{50}. For patients enrolled on St. Jude TOTXV or TOTXVI protocols LC_{50} was determined at St. Jude Children's Research Hospital. Publicly available data from European patients had been previously assayed in The Netherlands by MTT as previously described.[62] Patients from all cohorts were classified as resistant (≥ 64μM) or sensitive (<0.1 μM), according to previously described criteria [15]. For a subset of patients included in the whole exome sequencing mutation analysis who did not have prednisolone LC_{50} determined, their dexamethasone LC_{50} values were used after multiplying by a factor of eight to adjust for the difference in potency.

Gene expression by microarray

Total RNA was harvested from primary leukemia cells obtained from 203 patients at diagnosis using TRI Reagent (Molecular Research Center, Inc.). Gene expression was assessed in the Hartwell Center for Bioinformatics & Biotechnology at St. Jude Children's Research Hospital using either HG-U133A (GPL96) or HG-U133 Plus 2.0 (GPL570) microarray platforms (Affymetrix), according to the manufacturer's protocol. The "affy" Bioconductor R-project package or Affymetrix Microarray Suite version 5.0 [62,64,65] was used to implement the MAS5 algorithm for processing the gene expression data.

Gene expression by RNA Sequencing

Total RNA was harvested from 217 patients enrolled on St. Jude protocols (13 from St. Jude TOTXV, 176 from St. Jude TOTXVI and 26 St. Jude TOTXVII) and 103 adult patients (62

from the Eastern Cooperative Oncology Group, 32 from M.D. Anderson Cancer Center, 7 from the University of Chicago and 2 from the Alliance for Clinical Trials in Oncology), and total stranded RNA sequencing was performed. Total RNA was harvested from primary ALL samples using TRI reagent. In ALL cell lines, total RNA was isolated using the RNAeasy Mini kit (Qiagen), and stranded mRNA sequencing was performed. All RNA sequencing was carried out via the Illumina HiSeq platform by the Hartwell Center for Bioinformatics and Biotechnology at St. Jude Children's Research Hospital.

DNA methylation analysis

DNA was isolated from the bone marrow or peripheral blood of 178 newly diagnosed leukemia patients using the Blood and Cell Culture DNA kit (Qiagen). DNA methylation status was interrogated genome-wide using either the Infinium HumanMethylation27 BeadChip kit or the Infinium HumanMethylation450 BeadChip kit in accordance with the manufacturer's protocol (Illumina). HumanMethylation27 BeadChip experiments were performed at either the Emory Integrated Genomics Core (EIGC; Atlanta) or the Wellcome Trust Centre for Human Genetics Genomics Lab (Oxford).

HumanMethylation450 BeadChip experiments were performed at the Heflin Center for Genomic Science at the University of Alabama at Birmingham (Birmingham, Alabama, USA). Beta–values (β) [66] were derived from the raw output for each CpG site. Individual loci were grouped according to ENCODE criteria [29]; DNA methylation status was classified as: hypomethylated ($\beta \leq 0.2$), hemimethylated ($\beta > 0.2 < 0.6$) or hypermethylated ($\beta \geq 0.6$).

SNP analysis

DNA was extracted from ALL cells from bone marrow or peripheral blood samples from 184 newly diagnosed patients using the Blood and Cell Culture DNA kit (Qiagen). DNA samples were genotyped using the Affymetrix GeneChip Human Mapping 500K set or the SNP 6.0 array (Affymetrix). The arrays were scanned, and genotype calls were made using the BRLMM algorithm as implemented in the GTYPE software (http://www.affymetrix.com/products/software/specific/gtype.affx) as previously described [67]. SNPs were excluded for call rates of less than 95% amongst all patients or a minor allele frequency less than 1%. SNPs were annotated to genes for further comparative analysis between methods only if they were an expression quantitative trait locus (eQTL) as defined by Haploreg v 4.1.

miRNA expression analysis

Total RNA was extracted from ALL cells isolated from bone marrow or peripheral blood samples from 163 newly diagnosed patients. All microRNA expression microarrays were analyzed in the Hartwell Center for Bioinformatics & Biotechnology at St. Jude Children's Research Hospital, as previously described [68]. High-quality RNA was hybridized to miRCURY LNA 10.0 (GPL7722) generated from ready to spot probe sets or preprinted 6th generation miRCURY LNA microRNA microarrays (GPL11434) in accordance with the manufacturer's protocol (Exiqon, Woburn, MA). Upon removal of background signal data were log2 transformed and quantile normalized prior to analysis.

Whole Exome Sequencing Coding Variants

DNA was extracted from ALL cells isolated from bone marrow or peripheral blood from 201 newly diagnosed pediatric B-lineage leukemia patients using Blood and Cell Culture DNA kit (Qiagen). Alignment was performed to the reference human genome assembly GRCh37-lite with BWA and analyzed as previously described using matched germline sample as reference for somatic mutations.[69,70] Mutations were filtered for non-synonymous variants only in the coding region (excluding 3' and 5'UTR variants). They were then aggregated to individual genes and gene-level clustering via the Ward method was performed using Euclidean distance.

Hierarchical Clustering of Genomic Features

Each individual genomic feature type (mRNA, miRNA, DNA methylation, SNP, CNA and SNV/Indels) was rank ordered based by their linear regression p-values for association with prednisolone LC_{50}. Instanced hierarchical clustering was performed in a stepwise fashion beginning with the two most statistically significant probes. For each instance, Fisher's Exact Test (FET) was utilized to assess how well the clustered data could segregate resistant and sensitive leukemias when the highest clade of the dendrogram was split in two. Probes were added individually at each instance and hierarchical clustering and Fisher's Test calculations were repeated for up to 500 probes. Fisher p-values for the different patient cohorts were combined using meta-analysis (Stouffer's method) and the combination of probe sets that generated the lowest meta-analysis p-value was used as the signature for each individual feature type. 110,000 rounds of permutation were performed on the data to determine the likelihood that the observed meta clustering p-values for each feature was due to chance. Analyses were carried out in R using packages gtools, gdata, bitops, caTools, gplots, and amap. All data were clustered using the hcluster function in R using the "ward" method and distance used was "correlation" for all features except WES ("Euclidean") and SNPs ("binary"). All FDR corrected values were calculated using the Benjamini-Hochberg correction method for cutoffs of selected feature lists and can be found in Supplementary Table 1 for each respective feature type.

Connectivity among genomic features

To determine connectivity between mRNA expression and each of the other genomic feature types, we compared expression levels with each genomic feature type for all samples interrogated for both features.

Associations between DNA methylation and gene expression were deemed significant if there was a negative and statistically significant ($p < 0.05$) association according to linear regression (patient cohort included as a covariate), and the CpG site was within 100 kb of the gene's transcription start site. Connections between DNA methylation probes found to be inversely associated with expression of genes in the prednisolone resistance mRNA signature were included only if the methylation probe was also significantly associated with prednisolone LC_{50} ($p < 0.05$).

Connections between miRNA expression and gene expression were required to meet the following conditions: a negative association by linear regression (p-value < 0.05) and the

gene's transcript contains a miRNA binding site based in either of two *in silico* prediction databases (miRaNDA or miRDIP) or a database of experimental evidence of biological connection from public databases (mirTarbase).

Connections between SNPs, CNAs, SNVs/Indels and gene expression were required to have a linear regression p-value < 0.001 in both patient cohorts.

Genome-Wide CRISPR Knockout Screens

We transduced 12×10^6 NALM-6 human leukemia cells that were constitutively expressing Cas9 protein with either GeCKOv2 library A or B by spinfection for 2hr at 568g at an MOI between 0.3–0.5 to ensure only one gRNA per cell, as previously described [71]. Both libraries contained 6 gRNAs per gene and 1000 non-targeting controls and library A contained 4 gRNAs per miRNA. Cells were selected with 15ug/ml Blasticidin (Cas9) and 5ug/ml Puromycin (gRNA) to ensure that cells contained both gRNA and Cas9 protein. Representation of gRNAs was verified by sequencing the gRNA region using a two-step nested PCR reaction to amplify the region, as previously described.[20,71] For each library, 2×10^7 cells were treated with 100μM prednisolone for 72hr. After 72hr, viability of these cells ranged from 10–20% for all treatments. Cells were grown out until they reached >90% viability, and DNA was extracted using the Blood and Cell Culture Maxi kit (Qiagen). The gRNA region was sequenced via Illumina HiSeq 2500 using single reads in rapid run mode and gRNA enrichment/depletion analysis performed using the MaGeCK algorithm.[72,73] Genes that were not expressed based on RNA-seq of the NALM-6 cell line were removed from the analysis, and at least 4 significant ($p<0.005$) gRNAs were required to be included in the gene-level knockout reduced analysis. Gene level aggregation of gRNAs was performed using logit p-value transformation method in the R package metap. Effect sizes were calculated as Cohen's D.

Integrated Gene Level (TAP) Analysis

To assess a known gene's potential involvement in leukemia cell sensitivity/resistance to prednisolone, we combined evidence from all six genomic features within or in proximity to (50kb) every known human gene. Each genomic feature was evaluated individually for its association with prednisolone LC_{50}, features that were significant (linear regression $p<0.05$) were included in the overall gene level model. A hybrid permutation approach was used along with a non-parametric smooth CDF (cumulative distribution function) with a variation diminishing spline to obtain a TAP (Truncated Aggregation of P-values) statistic for every gene [74,75]. Adaptive thresholding was used, as previously described to define the threshold of significance [76]. Genes meeting this threshold were used to select top candidate genes for further analysis (see Supplemental Notes).

Single Cell RNA sequencing

To interrogate the expression of genes at the single cell level in patients who were either sensitive or resistant to prednisolone *in vitro*, primary patient ALL cells were collected at diagnosis and incubated for 96 hours with or without prednisolone. Patient cells were re-suspended at a concentration of 2×10^6 cells/mL in culture media, as described above. On day zero, 80 μL of cells were plated in round bottom 96-well plates. Cells were incubated

for 4 days with either 63μM prednisolone or no drug, collected and washed with 50 μL of PBS and 150μL total volume was collected. Both control and treated samples were processed and subjected to single cell RNA-sequencing on the 10x Genomics platform. The Cellranger software from 10x Genomics was used to demultiplex each of the samples, align the demultiplexed reads to the hg19 human genome, collapse PCR duplicate reads into UMIs, and generate a matrix of UMI counts for each cell and Ensembl ID combination.

All UMIs aligning to ribosomal protein-coding or mitochondrial genes were removed from the count matrices. Cells were removed if less than 500 genes were detected from the remaining UMIs. UMI counts within a cell were normalized by dividing each UMI count by the total UMI count across the cell, scaling by the median total UMI count across all cells from the four samples, adding a pseudocount of one, and taking the natural logarithm.

PCA was performed jointly on control and treatment samples from each patient. The first 40 principal components of overdispersed genes were used to generate a two-dimensional embedding of cells using the Barnes-Hut implementation of tSNE with a perplexity of 30 [77]. Dispersion was calculated as described elsewhere [78] and as implemented in Seurat (https://github.com/satijalab/seurat), with overdispersed genes being genes in each bin that have z-scores at or above 1.4 (n = 922 genes for sensitive and n=663 for resistant).

Cell-cell Euclidean distance matrices were computed jointly for control and post-treatment samples of each patient using the over-dispersed genes. Hierarchical clustering of the cells using the Euclidean distance matrix was performed using the Ward method [79]. Clusters were then identified using DynamicTreeCut, an iterative cluster partitioning and agglomeration method.

Clusters with at least 20% of the component cells expressing CD19 were classified as B cells. The null hypothesis that the proportion of CD19+ cells between control and treatment samples for each patient was tested using the prop.test function in R, and differential expression of genes was tested using the Wilcoxon rank sum test as implemented in the Seurat R package. This resulted in seven clusters for the resistant patient and eleven clusters from the sensitive patient (Extended Data Fig. 8 a, d). Clusters of the B-lineage leukemia cells were identified based on the expression of *CD19* in the component cells. Other cell types were identified by identifying the most highly differentially expressed genes in each cluster that are known markers of hematopoietic lineage (e.g. T-cells, red blood cells; Extended Data Fig. 8b, e). The sensitive patient in our single cell analysis had a B-lineage ALL with P2RY8-CRLF2 fusion. The resistant patient in this analysis had a BCR-ABL positive B-lineage ALL.

Immunoblot

Cells were pelleted at 500xg. Lysates were prepared in RIPA buffer (Sigma-Aldrich) containing cOmplete Protease Inhibitor Cocktail (Roche Life Science) and PhosStop (Sigma-Aldrich). Equivalent amounts of extract (20 μg) were separated on 3–8% Novex Tris-Acetate polyacrylamide gels (Thermo Fisher Scientific) and transferred to polyvinylidene fluoride (PVDF) membranes (0.2 μm). Non-specific binding was blocked with 5% Milk in TBS with 0.05% Tween-20 for at least 1hr prior to incubation of

membranes with primary and secondary antibodies. Primary antibodies used were rabbit anti-CELSR2 monoclonal (Cell Signaling; D2M9H) diluted 1:1,000, mouse anti-BCL2 monoclonal (Cell Signaling;124) diluted 1: 1,000, mouse anti-BIM monoclonal(Cell Signaling;C34C5) diluted 1:1,000, mouse anti GR(BD Biosciences; #611227) diluted 1:1,000, mouse anti p-JNK (Santa Cruz Biotech; sc-6254) diluted 1:500, rabbit anti cJun (Cell signaling; 9165), rabbit anti phospho-cJun Ser63 (Santa Cruz Biotechnology; sc-822) diluted 1:500, rabbit anti NFAT1 (Cell Signaling; 4389) diluted 1:1,000, SAPK/JNK (Cell Signaling; 9252) diluted 1:1,000, mouse anti GAPDH (Santa Cruz Biotechnology; sc-47724), mouse anti PAX5 (Cell Signaling; 12709) diluted 1:1000mouse anti BCL2 (Cell Signaling; 15071) diluted 1:1000, mouse anti glucocorticoid receptor (BD Biosciences; 611227) diluted 1:1000 rabbit anti LaminB1 (Cell Signaling; 12586) diluted 1:1000 and anti-β-actin (Sigma-Aldrich; A5441) diluted 1:100,000. Membranes were then incubated with appropriate HRP-Conjugated IgG secondary antibodies (Jackson Immunoresearch) and developed with SuperSignal West Femto chemiluminescent substrate (Thermo Fisher Scientific) prior to signal acquisition using an Odyssey Fc Imager (LI-COR). Image processing and signal quantification were performed with Image Studio software (Version 4.0; LI-COR). Nuclear/Cytoplasmic protein extraction was performed using the NE-PER Nuclear and Cytoplasmic Extraction kit (ThermoFisher) using standard protocol.

ChIP-seq and ATAC-seq

ChIP-seq was performed as previously described [80]. Briefly, 20 million NALM-6 cells were crosslinked using 1% formaldehyde and sonicated on a Diagenode Bioruptor Plus sonicator. Chromatin immunoprecipitation was performed using 5μg anti-PAX5 antibody (Abcam, ab15164). ChIP-seq and input control libraries were run on an Illumina HiSeq4000 next-generation sequencing machine using single-end 50bp sequencing, reads were mapped to the hg19 reference genome using BWA and binding sites were called using MACS2 peak caller. ATAC-seq was performed using the Fast-ATAC protocol[81]. Briefly, 10,000 cells were transposed in a cocktail containing 1% digitonin. Following transposition, DNA was collected using the Qiagen MinElute Reaction Cleanup Kit (Qiagen #28204) and amplified for 5 cycles using barcoded Nextera PCR primers. A quantitative PCR reaction was performed on an Applied Biosystems QuantStudio 3 Real-Time PCR machine using 5uL of PCR product to determine the additional number of PCR cycles required. PCR products were subsequently re-amplified for the appropriate number of additional PCR cycles and DNA was size-selected using SPRIselect beads (Beckman Coulter, B23317). ATAC-seq libraries were run on an Illumina HiSeq4000 next-generation sequencing machine using paired-end 100bp sequencing, reads were mapped to the hg19 reference genome using Bowtie2 and open chromatin sites were called using the MACS2 peak caller.

Previously Reported Mechanisms of Prednisolone Resistance

To assess the performance of our agnostic polygenomic method to identify genes that confer resistance to glucocorticoids, we used Illumina BaseSpace® Literature Correlation Engine to perform a literature search to identify all genes previously reported to confer resistance to glucocorticoids (performed January 2018). The search terms “glucocorticoids, leukemia” were used for our initial search, with a secondary filter of “resistance”. This resulted in 426 total publications, which we narrowed using the “genes and proteins” tab set on the “top

1000” setting and exporting the list of top word cloud tags that were found from our search. This list of word cloud tags was entered into the HUGO database (https://www.genenames.org/cgi-bin/symbol_checker); the resulting list was trimmed by removing unmatched terms. This generated a list of 347 unique genes published through 2016. We also included genes published in papers from January 2017-January 2018 that were found by a PubMed search using search terms “glucocorticoids, resistance, leukemia” with results limited by publication date, yielding 27 additional publications. For all genes included in our tabulation of known genes previously associated with glucocorticoid resistance, we required a published report linking the gene to poor patient response (i.e. remission induction failure, persistence of minimal residual disease [MRD], or disease relapse) or glucocorticoid resistance as measured in primary ALL cells and that the gene/pathway was confirmed through either direct manipulation or chemical inhibition in a human cell culture model or patient derived xenograft (PDX). Using the aforementioned methods and criteria, a table of “known mechanisms” was generated (Supplementary Table 7) and comparisons were then made to genes identified as significantly related to glucocorticoid resistance by our three methods (polygenomic, TAP, CRISPR screening), using either all genes identified by any one of these methods or using the subset of genes identified by two or more of these methods. Direct matches of genes were considered the strongest evidence. Genes that were not directly matched were considered to have an associated pathway component if they were found by searching for the gene in STRINGdb with the following criteria: 1) Only 30 first shell interactors with a correlation > 0.7 (high confidence), 2) only “Text-mining”, “Experiments”, “Databases”, “Co-expression” were used to define informative data sources. In all cases, concordance of directionality of the relationship was required between published genes and those discovered in our analyses.

NetBID analysis to identify drivers of GC-resistance in ALL patients

We applied the network-based integrative NetBID[82] algorithm to identify “hidden” drivers in GC-resistant primary leukemia cells (ALL cells from patients) using gene expression profiles. We first reverse-engineered a B-ALL specific interactome (BALLi) from TARGET[26] RNA-Seq data from 185 B-ALL primary leukemia cells against 1,673 transcription factors and 6,247 signaling proteins. The data-driven BALLi resulted in 21,655 nodes and 830,213 edges. Then we applied NetBID (signed=TRUE) on comparisons of resistant (level=3) versus sensitive (level=1) ALL cells and separately for intermediate (level=2) versus sensitive ALL cells from two cohorts of patients enrolled on St. Jude TOTXV or TOTXVI clinical trials. We removed the batch effects from TOTXV cohort by using the “removeBatchEffect” function in limma. We also integrated driver results from TOTXV and TOTXVI patients using two different microarray platforms (HG-U133A and HG-U133_Plus_2). The top 48 drivers were selected by the following criteria: network size > 50, $p < 5\times10^{-5}$ in TOTXVI and integrated (combined) analysis of highly-resistant vs. sensitive patients, and that the intermediate vs. sensitive and the resistant vs. sensitive results were concordant. Further information regarding the NetBID analysis can be found in Supplemental Notes and the NetBID package can be found online at: https://github.com/jyyulab/NetBID.

Drug synergy experiments and response surface modeling

Relationship of response was determined when prednisolone was given alone or in combination with three concentrations of venetoclax using both NALM-6 cells (10nM, 100nM, 1μM) and 697 cells (1nm, 10nm, 50nm). Concentration ranges of venetoclax differed because of differences in sensitivity to venetoclax between the two cell lines. Viability assays were carried out using Cell Titer Glo. In synergy experiments with primary leukemia cells from patients, 1nM, 10nM and 100nM concentrations of venetoclax were used to assess synergy with prednisolone. Synergy was assessed by response surface modeling method for full details see Supplemental Notes.

Flow cytometry

Blood was collected from the retro-orbital sinus, facial vein, or tail vein of anesthetized mice to assess engraftment of human ALL cells. Blood was lysed with the BD FACS Lyse Wash Assistant (BD Biosciences, San Jose, CA). Cells were stained with antibodies to human CD19 (eBioscience;45–0199-42, PerCP-Cy 5.5) and mouse CD45 (Tonbo; 20–0451-U100, APC). Samples were assayed on the BD LSR II or LSR Fortessa (BD Biosciences) and analysis was performed with FlowJo version 10 (FlowJo, LLC, Ashland, OR).

In vivo drug combination studies

NALM-6 cells were injected into non-irradiated 8–12 week old female NSG mice (100,000 cells/mouse). Treatment was started three days post injection and continued until the endpoint was reached for each mouse. Mice were treated with either continuous dexamethasone (4mg/L) alone, venetoclax alone (50 or 100mg/kg), as previously described [83] or either dosage of venetoclax in combination with dexamethasone. Dexamethasone was given daily in drinking water with tetracycline (1g/L; Sigma-Aldrich, St. Louis, MO), and half of each week the water contained Sulfamethoxazole (600 mg/L) and trimethoprim (120mg/L; from Hi-Tech Pharmacal, Amityville, NY). Mice were randomized following injection. Mice were sacrificed when they became moribund for any reason, as determined by the veterinarian.

Statistics & Reproducibility

All statistical analyses were performed using R software or Graphpad Prism 8 unless otherwise stated. For box plots unless stated explicitly, upper and lower values in each box depict the 75th and 25th percentiles, respectively, the solid line represents the median, and the top and bottom of each dashed vertical line depict the most extreme data points that were no more than 1.5 times the interquartile range (75th percentile–25th percentile) from the box. All bar plots are representing mean ± standard deviation (S.D.) and each dot represents and independent experiment or sample. For all analyses comparing means of groups student's t-test was performed, Chi-Squared analysis was used for MRD group data, linear model was used as the predominant method for statistical significance in genome-wide analyses using LC_{50} as a continuous variable and Fisher's tests were used to describe clustering of genomic data vs LC_{50}. Customized methods were also used such as NetBID which relied on Bayesian inference and used z-scores to report significance[25] and the TAP

method which utilized a hybrid permutation and an adaptive thresholding approach to assessing statistical significance of higher order problems.

Data Availability

DNA methylation, gene expression and ChIP-seq data are available at the Gene Expression Omnibus (GEO) under accession GSE66708. miRNA data can be found at GEO under the accession number GSE76849. Cell line RNA-seq data can be found at GEO under the accession number GSE115384. Validation cohort #1 RNA-seq data from 73 of the 320 patients in the independent second cohort can be found at GEO under the accession GSE115525. Additional RNA-seq data from validation cohort #1 (n= 247) can be found at GEO under GSE124824. PAX5 CHIP-seq can be found at GEO under the accession GSE115764. Cell line ATAC-seq data can be found at GEO under the accession GSE129066. Genotype data can be found in dbGaP at https://www.ncbi.nlm.nih.gov/projects/gap/cgi-bin/study.cgi?study_id=phs000638.v1.p1. Source data has been provided in the form of unprocessed images for all western blots (Figures 3,4 and 7 and Extended Data Figures. 4,7 and 9) and for graphs (Figures 1,3,4 and 5,8 and Extended Data Figures. 4,5,7 and 9) in the manuscript. All other data supporting the findings of this study are available from the corresponding author upon reasonable request.

Code availability

Code used to generate for the polygenomic analysis and the TAP analysis can be found on GitHub at https://github.com/evanslabSJCRH/Polygenomic-Analysis. The NetBID code can be found at https://github.com/jyyulab/NetBID. Any custom code generated for our analyses not specifically listed here or in the text may be requested from Dr. William E. Evans (William.Evans@stjude.org). All R packages or other software used are listed in methods section for each relevant analysis.

Extended Data

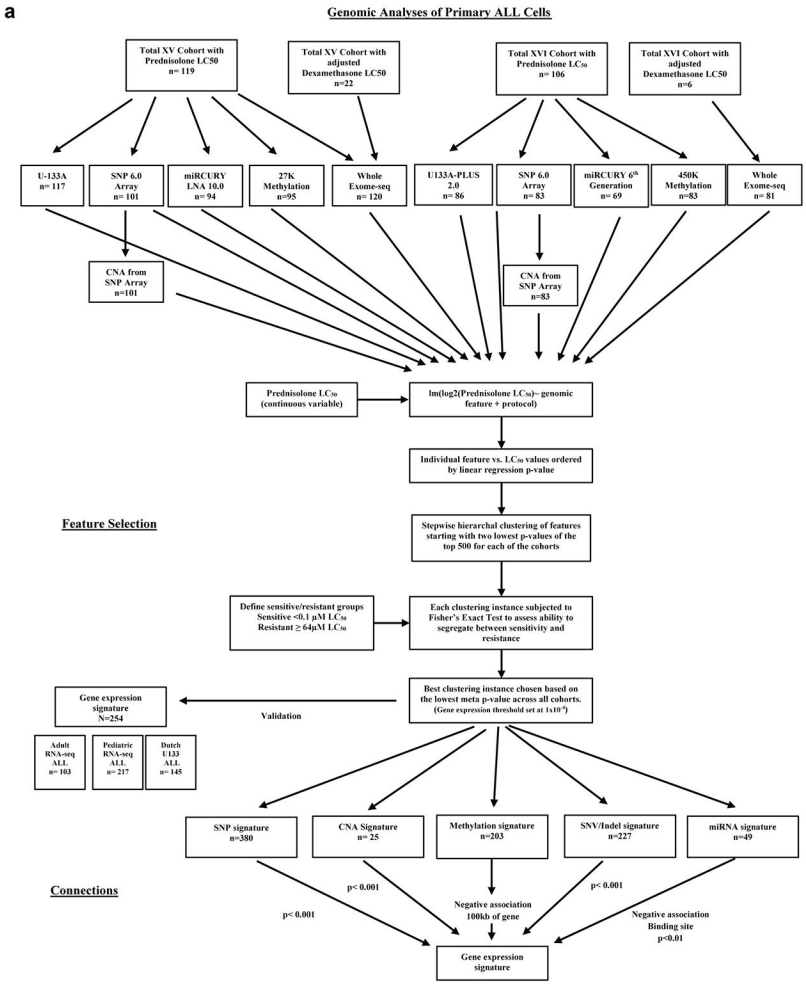

b

Variable	Levels	n_{TOTXV}	$\%_{TOTXV}$	$\Sigma\%_{TOTXV}$	n_{TOTXVI}	$\%_{TOTXVI}$	$\Sigma\%_{TOTXVI}$	n_{all}	$\%_{all}$	$\Sigma\%_{all}$
Age > 10	>= 10	16	18.8	18.8	20	18.9	18.9	36	18.9	18.9
	< 10	69	81.2	100.0	86	81.1	100.0	155	81.2	100.0
p = 1.00	all	85	100.0		106	100.0		191	100.0	
Sex	Female	64	53.8	53.8	52	49.1	49.1	116	51.6	51.6
	Male	55	46.2	100.0	54	50.9	100.0	109	48.4	100.0
p = 0.51	all	119	100.0		106	100.0		225	100.0	
Race	White	80	67.8	67.8	64	61.0	61.0	144	64.6	64.6
	Black	17	14.4	82.2	16	15.2	76.2	33	14.8	79.4
	Hispanic	17	14.4	96.6	14	13.3	89.5	31	13.9	93.3
	Asian	1	0.8	97.5	0	0.0	89.5	1	0.5	93.7
	Other	3	2.5	100.0	11	10.5	100.0	14	6.3	100.0
p = 0.11	all	118	100.0		105	100.0		223	100.0	
Molecular Subtype	B-other	26	21.9	21.9	24	22.6	22.6	50	22.2	22.2
	Hyperdiploid	27	22.7	44.5	25	23.6	46.2	52	23.1	45.3
	Hypodiploid	9	7.6	52.1	4	3.8	50.0	13	5.8	51.1
	Ph-like	4	3.4	55.5	5	4.7	54.7	9	4.0	55.1
	Ph-like-CRLF2	4	3.4	58.8	1	0.9	55.6	5	2.2	57.3
	BCR-ABL	2	1.7	60.5	2	1.9	57.5	4	1.8	59.1
	CRLF2-non-Ph-like	1	0.8	61.3	3	2.8	60.4	4	1.8	60.9
	TCF3-PBX1	8	6.7	68.1	5	4.7	65.1	13	5.8	66.7
	ETV6-RUNX1	27	22.7	90.8	30	28.3	93.4	57	25.3	92.0
	MLL-AF4	3	2.5	93.3	4	3.8	97.2	7	3.1	95.1
	ERG	8	6.7	100.0	3	2.8	100.0	11	4.9	100.0
p = 0.70	all	119	100.0		106	100.0		225	100.0	

Extended Data Fig. 1. Polygenomic analysis workflow

(a.) Flowchart depicting cohorts, genomic assays and detailed analysis pipeline for polygenomic analyses of multiple feature types (mRNA, miRNA, DNA methylation, SNVs, CNVs and WES mutations) as determinants of prednisolone sensitivity in patients diagnosed with acute lymphoblastic leukemia ("lm" = linear model). **(b.)** Table describing age, race, gender and molecular subtype of discovery cohort (n=225 patients) from polygenomic

analysis. The P-values represent differences between the discovery cohort enrolled on the two clinical trials (Fisher's Exact Test p-value; Total 15 and Total 16).

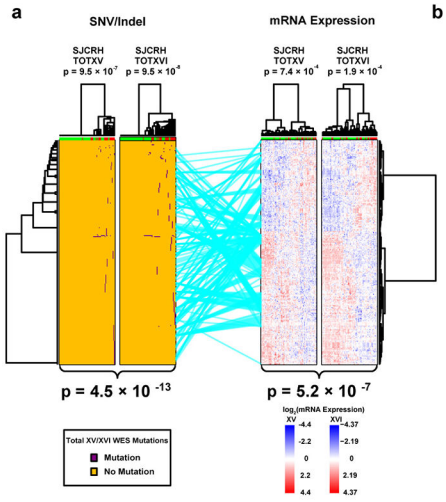

b

Gene	Class	Amino Acid Change	Statistic	PRED LC_{50} p-value	CADD Score	SIFTcat
MLL2	nonsense,missense, missense	Q5365*(1), L4992M (1), Q3611K(1)	2.84	0.007	47, 25, 24	NA,Del,Del
CXorf30	splice_region, missense	S455_E15splice_region (1), T293M (1)	3.32	0.010	1.8, 0.001	NA, Tol
ZSCAN20	missense, missense	C399F(1),N264I(1)	3.32	0.010	28.8, 1.2	Del, Tol
KRAS	missense, missense,missense, missense,missense, missense,missense, missense	A146P(1),A146T(2),D119H (1),A18D(1),Q61L,G12S(1) ,T58I(1),L19F(1),G13D(6), G12D(8), Q61H(1)	0.85	0.013	32,32,30,28.9,27. 5,27,25.9,25.7,24 .6,24.5,24	NA,Del,NA Del, Del, NA,Del,Del Del, Del
RACGAP1P	exon,exon	E1_exon(2)	3.08	0.017	13, 10.6	NA
ADCY8	missense, missense	R1227W(1),V247M(1)	3.01	0.019	34,17.7	Del,Tol
KEL	missense, missense	R447W(1),F69L(1)	2.90	0.024	24.1, 13.5	Del,NA
KANK4	nonsense, missense	E329*(1), D147N(1)	2.88	0.026	36,13.6	NA,Tol
KIAA1486	missense,missense	E269K(1),T419M(1)	2.88	0.026	33,23.8	Del,Del
COL25A1	missense,missense	R364W(1),R618H(1)	2.82	0.029	33,33	Del,Del
ABCA6	missense,missense,mis sense	L1510V(1),L330F(1), E814D(1)	-2.20	0.038	23.3,13.8,6.8	Del,Tol,Tol
SEZ6L2	missense,missense	G666W(1),E763K(1)	2.58	0.046	32,22	Del,NA
ERG	missense,missense	A368P(1),D363A(1)	2.53	0.050	29.4, 29.3	Del,Del

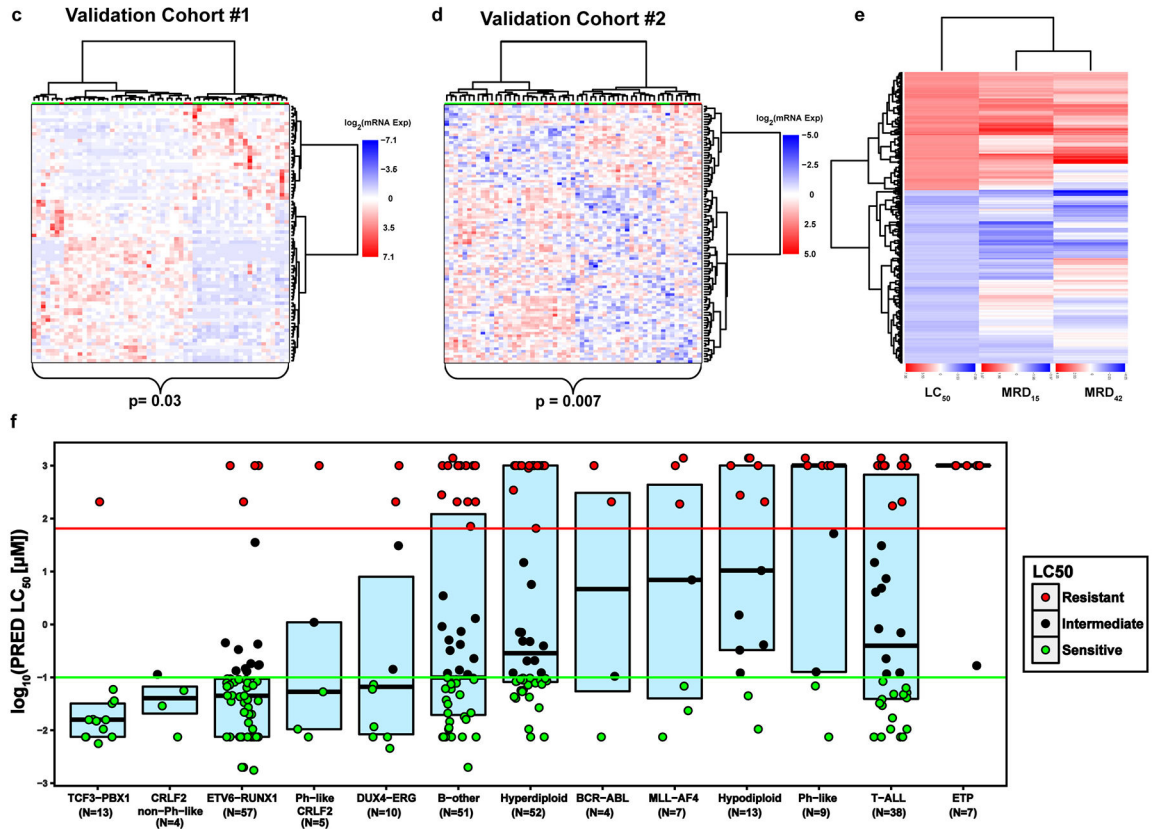

Extended Data Fig. 2. Validation of gene expression signature, relation to treatment response and WES variant connectivity

(a.) Connectivity between polygenomic signatures for mutation (n=227 mutations) and mRNA expression (n=254 mRNA probes; Fisher's Exact Test clustering p-values and linear model p-value for connectivity). **(b.)** Characteristics of WES mutations with linear model p-value <0.05 vs. LC_{50}. (SIFTcat Del = Deleterious and Tol = Tolerated). **(c.)** RNA sequencing

of ALL cells from St. Jude Total XVI patients (n=73 patients; validation cohort #1; Fisher's Exact Test clustering p-value) clustered with gene expression signature from discovery cohort analysis. **(d.)** Publicly available DCOG/COALL patient cohort (n=145 patients; validation cohort #2; Fisher's Exact Test clustering p-value) clustering with gene expression signature from patient discovery cohort. **(e.)** Clustering of gene expression vs. LC_{50}. Red denotes genes correlated with LC_{50} or minimal residual disease (MRD) in positive direction. Blue denotes genes correlated in negative direction with LC_{50} or MRD. Clustering performed to show concordance of genes discriminating LC_{50} or MRD. **(f)** Boxplot denoting Prednisolone LC_{50} in patients from discovery cohort with the major ALL molecular subtypes. Red circles denote prednisolone resistant patients, green denotes sensitive patients, and black denotes intermediate sensitivity. Upper line is the upper quartile (75%) middle line is the median and lower line is lower quartile (25%) boundary for Prednisolone LC_{50}.

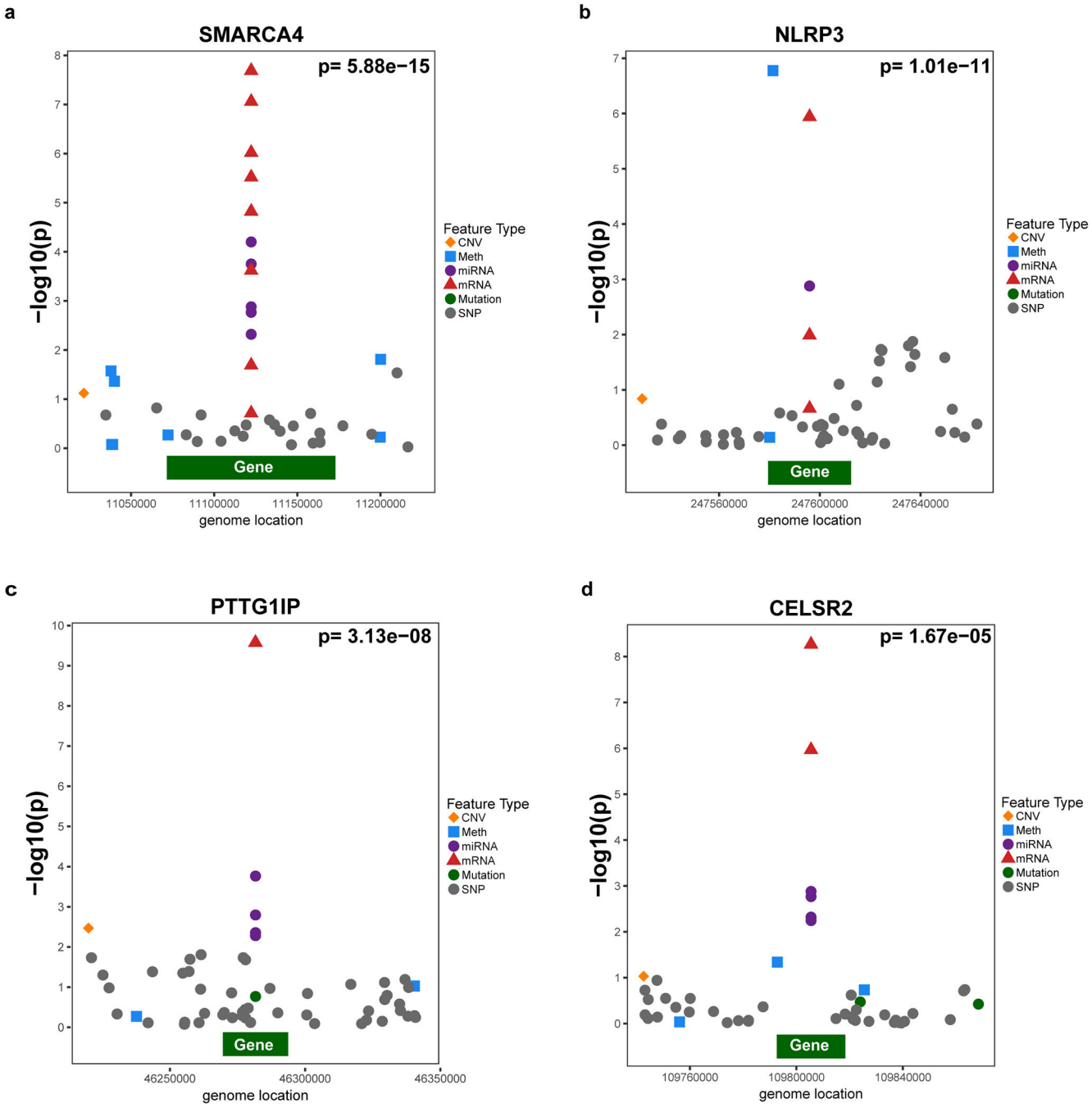

Extended Data Fig. 3. Gene level integration of genomic variants related to prednisolone resistance

Each panel depicts -log10 p-values for the association of the indicated genomic feature with prednisolone LC_{50}, and the aggregated gene-level linear model p-value based on all genomic features is shown for each gene at the top right. Red triangles represent mRNA probes within the gene body, orange diamonds depict copy number variants, blue squares are DNA methylation probes, grey circles SNVs, and purple circles miRNAs within 50kb upstream or downstream of gene region (n=203 patients). **(a.)** *SMARCA4*, a component of the SWI/SNF

complex, has been previously linked to glucocorticoid resistance in pediatric ALL[19] **(b.)** *NLRP3* encodes NALP3, an inflammasome component that activates caspase 1, and has been previously associated with ALL resistance to glucocorticoids.[15] **(c.)** *PTTG1IP* encodes the pituitary tumor-transforming gene 1 proteininteracting protein that interacts with the proto-oncogene *PTTG1* (also known as securin). **(d.)** *CELSR2* is a G-protein coupled receptor involved in non-canonical Wnt signaling. *PTTG1IP* and *CELSR2* are novel genes from the current study associated with glucocorticoid resistance.

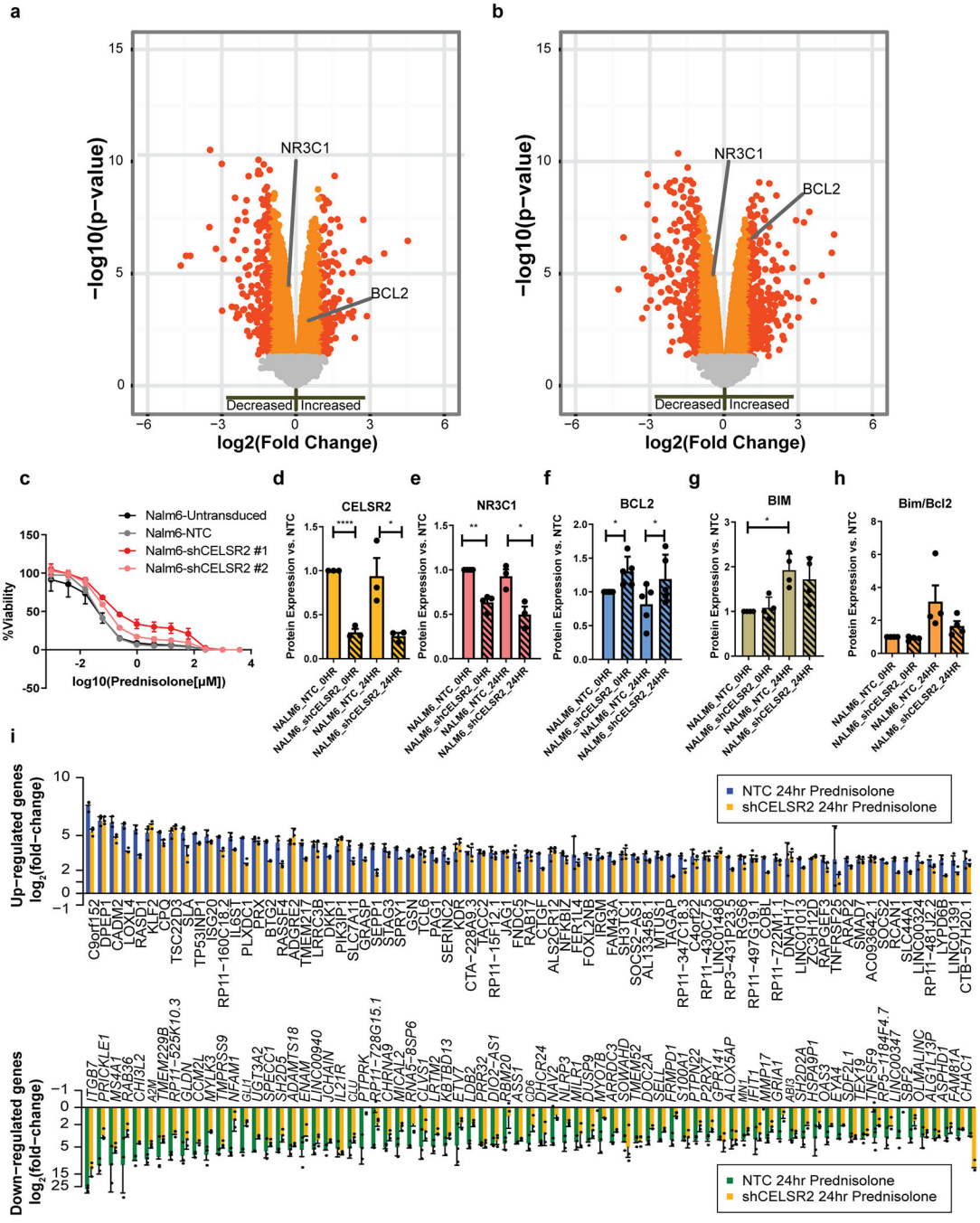

Extended Data Fig. 4. *CELSR2* knockdown blunts glucocorticoid responsiveness of 697 cells and increases sensitivity to venetoclax

(a.) Volcano plot for untreated *CELSR2* knockdown ALL cell lines vs. non-target control in 697 cell line (n= 3 independent experiments; linear model p-value). Left side of plot depicts genes with reduced expression in *CELSR2* knockdown cells and genes to the right had increased in expression in *CELSR2* knockdown cells. **(b.)** Volcano plot of gene expression after 24 hours of prednisolone treatment of *CELSR2* knockdown vs. non-target control ALL cells (697; n= 3 independent experiments; linear model p-value). **(c.)** Dose-response plot (mean ± S.D.; n= 3 independent experiments) of two shRNA constructs vs non-targeting control and un-transduced NALM-6 leukemia cell line. **(d.)** CELSR2 (n= 3 independent experiments) **(e.)** *NR3C1* (n= 4 independent experiments) **(f.)** *BCL2* (n=5 independent experiments) **(g.)** *BIM* (n= 4 independent experiments) *and* **(h.)** *Bim/Bcl2* protein expression (mean ± S.D; n=4 independent experiments; two-tailed t-test p-values; * =p < 0.05, ** = p <0.01, *** = p <0.001, **** = p <0.0001) in NALM-6 cells comparing controls (NTC; solid bars) to *CELSR2*-knockdown (shCELSR2) either prior to prednisolone treatment (0HR) or after 24hr prednisolone treatment (24HR). **(i.)** The 75 most highly upregulated (top) or downregulated (bottom) genes after 24 hours treatment with 10μM prednisolone. Blue and green bars depict mRNA expression (mean ± S.D.; n= 3 independent experiments) in 697 cells transfected with non-target control vector and gold bars depict cells expressing shRNA for *CELSR2* knockdown.

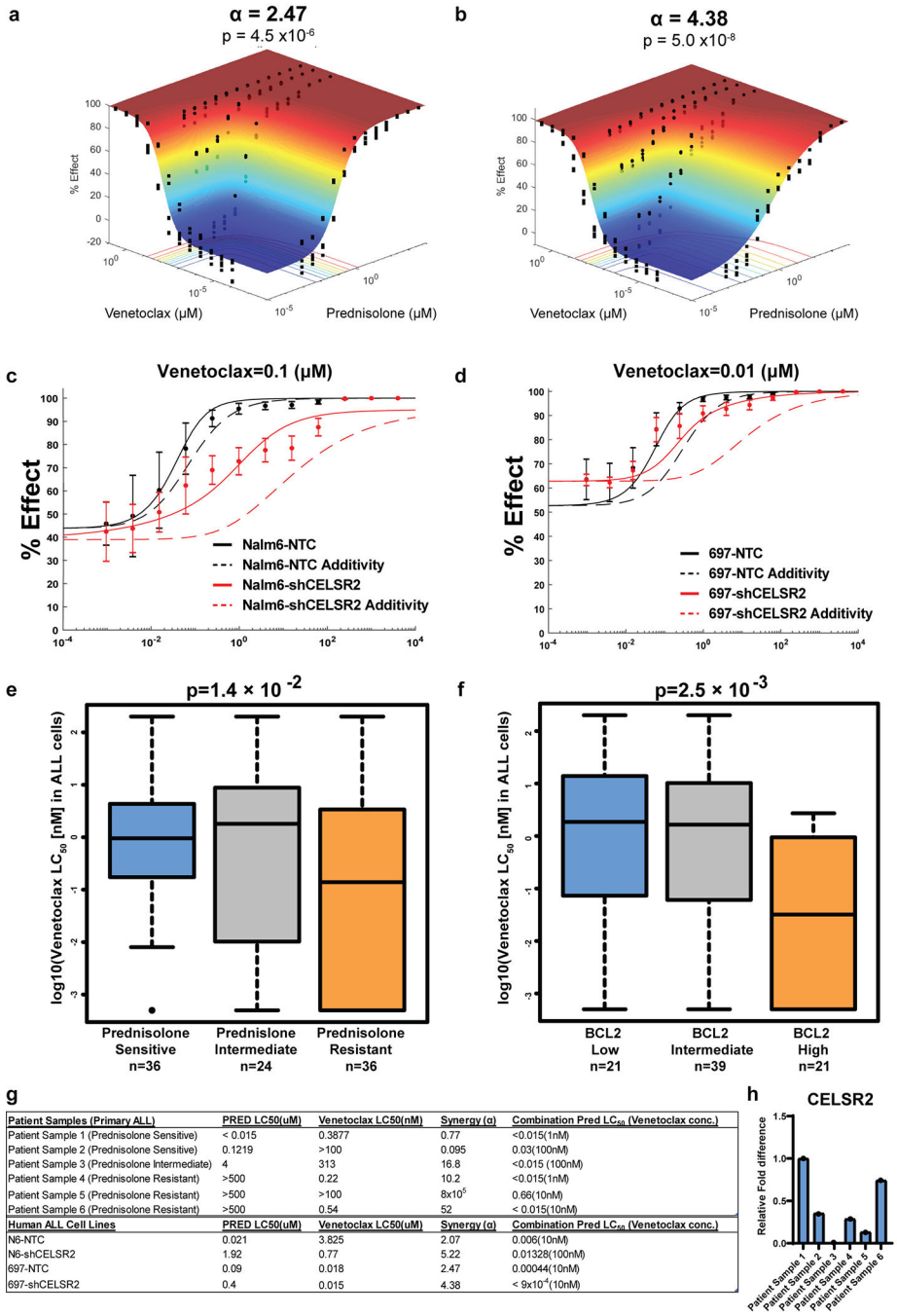

Patient Samples (Primary ALL)	PRED LC50(uM)	Venetoclax LC50(nM)	Synergy (α)	Combination Pred LC_{50} (Venetoclax conc.)
Patient Sample 1 (Prednisolone Sensitive)	< 0.015	0.3877	0.77	<0.015(1nM)
Patient Sample 2 (Prednisolone Sensitive)	0.1219	>100	0.095	0.03(100nM)
Patient Sample 3 (Prednisolone Intermediate)	4	313	16.8	<0.015 (100nM)
Patient Sample 4 (Prednisolone Resistant)	>500	0.22	10.2	<0.015(1nM)
Patient Sample 5 (Prednisolone Resistant)	>500	>100	$8x10^5$	0.66(10nM)
Patient Sample 6 (Prednisolone Resistant)	>500	0.54	52	< 0.015(10nM)
Human ALL Cell Lines	**PRED LC50(uM)**	**Venetoclax LC50(uM)**	**Synergy (α)**	**Combination Pred LC_{50} (Venetoclax conc.)**
N6-NTC	0.021	3.825	2.07	0.006(10nM)
N6-shCELSR2	1.92	0.77	5.22	0.01328(100nM)
697-NTC	0.09	0.018	2.47	0.00044(10nM)
697-shCELSR2	0.4	0.015	4.38	< $9x10^{-4}$(10nM)

Extended Data Fig. 5. Venetoclax and prednisolone synergize in primary ALL with low *CELSR2* expression and *CELSR2* knockdown in cell lines disregulation of Bim/Bcl2 axis

(a.) Response surface model plot of cytotoxicity from prednisolone plus venetoclax at concentrations indicated for the 697 leukemia cell line transduced with non-targeting control vector. **(b.)** Response surface model plot for the 697 leukemia cell line transduced with *CELSR2* shRNA knockdown vector (for a and b individual points represent n= 3 independent experiments performed in technical duplicate; response surface model two-tailed t-test p-value). The alpha (α) value indicates antagonism < 0 or synergy > 0 with

greater synergy from higher value. P-value describes overall model fit. Individual plots of prednisolone effect (mean ± S.D.; n= 3 independent experiments) **(c.)** NALM-6 and **(d.)** 697 leukemia cell lines at one concentration of venetoclax (mean ± S.D.; n= 3 independent experiments). Black lines are non-targeting control cells and red lines are *CELSR2* knockdown cells, dashed lines indicate predicted additivity curve fit based on single drug treatments; data left of the dashed lines represent additivity/synergy. Solid lines represent fit of measured values. **(e.)** Venetoclax sensitivity of independent cohort of patients (n=96 ALL patients) grouped based on prednisolone sensitivity (LC_{50}) **(f.)** Bcl2 expression associated with sensitivity to venetoclax (n= 81 ALL patients) **(g.)** Primary ALL cells from patients (n=6 patient samples) and human leukemia cell lines assessed for additivity/synergy with prednisolone and venetoclax (for all box plots horizontal bars depict medians and boxes represent 25^{th} and 75^{th} percentiles, whiskers represent ±1.5x IQR; linear model p-values). **(h.)** mRNA expression (n=1 experiment run in technical triplicate) of *CELSR2* in patient samples assessed for synergy.

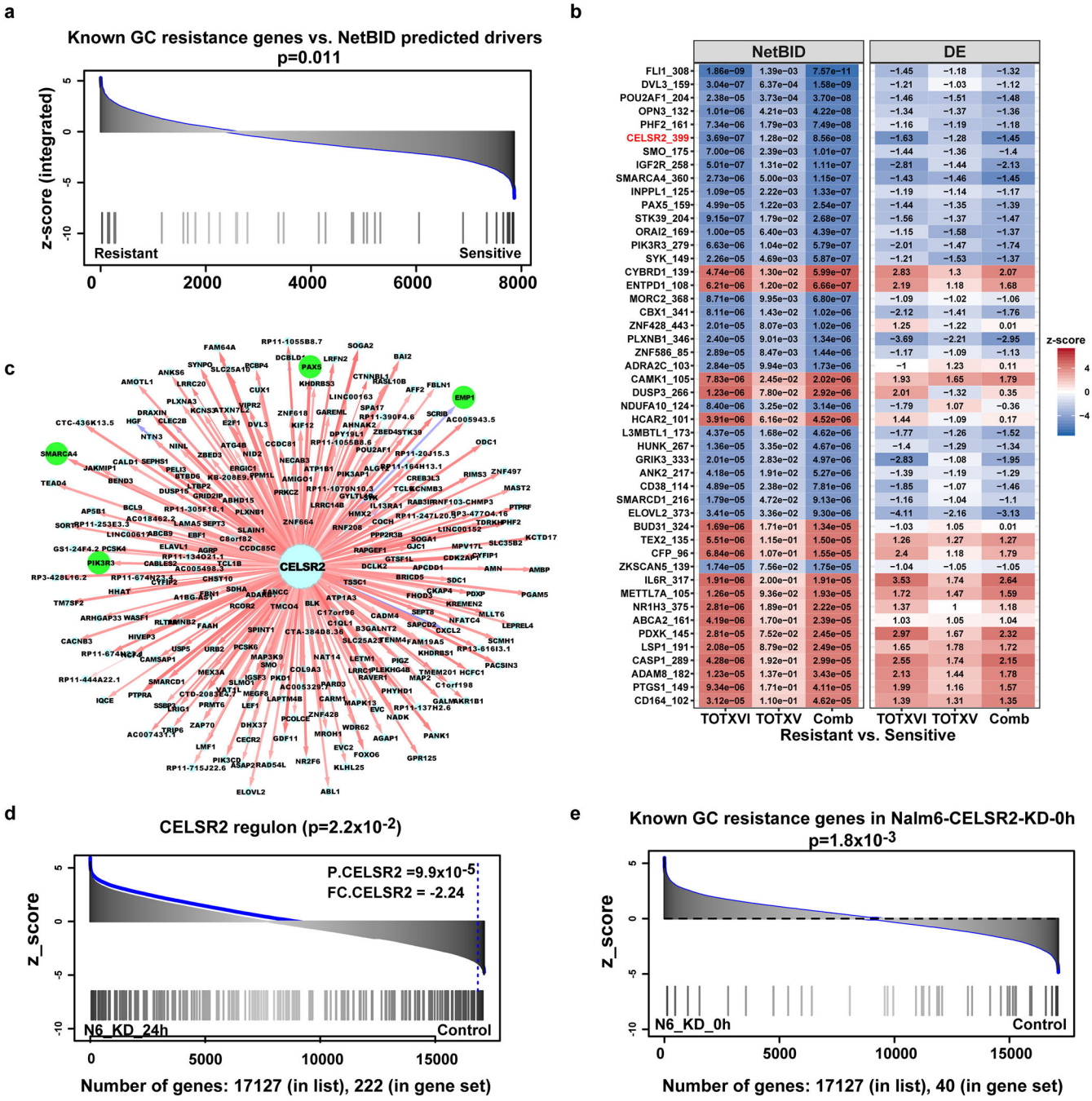

Extended Data Fig. 6. NetBID identifies regulatory nodes of prednisolone resistance

(a.) Enrichment of previously reported resistance genes (n=40 genes and miRNAs; Wilcoxon two-tailed p-value) in NetBID results. **(b.)** Heatmap of top 48 NetBID-predicted drivers ('symbol'_'regulon size') are ranked by integrated NetBID p-value. Left: color-coded by z-score and labeled by p-value of NetBID results in TOTXVI, TOTXV, and combination (Comb); Right: differential expression of each driver itself, color-coded by z-score and labeled by signed fold-change in TOTXVI, TOTXVI and combination (Comb; (Stouffer's combined Bayesian generalized linear model "NetBID" p-value; n=203 patients).

(c.) *CELSR2* regulon from B-ALLi (n=399 genes). Legends of node and edge follow Figure 6c. **(d.)** Enrichment of NetBID-inferred *CELSR2* regulon (n=399 genes) in differentially expressed genes of *CELSR2* knockdown vs. NTC in Nalm-6 human ALL cell lines (n=222 genes; Wilcoxon two-tailed p-value) upon prednisolone treatment for 24hr (top) Blue lines inside the box indicate the down-regulation of *CELSR2* itself, labeled p-value and signed foldchange. **(e.)** Enrichment of previously reported resistance genes (n= 40 genes and miRNAs; Wilcoxon two-tailed p-value) in differentially expressed genes of *CELSR2* knockdown vs. NTC in NALM-6 ALL cell lines without prednisolone treatment.

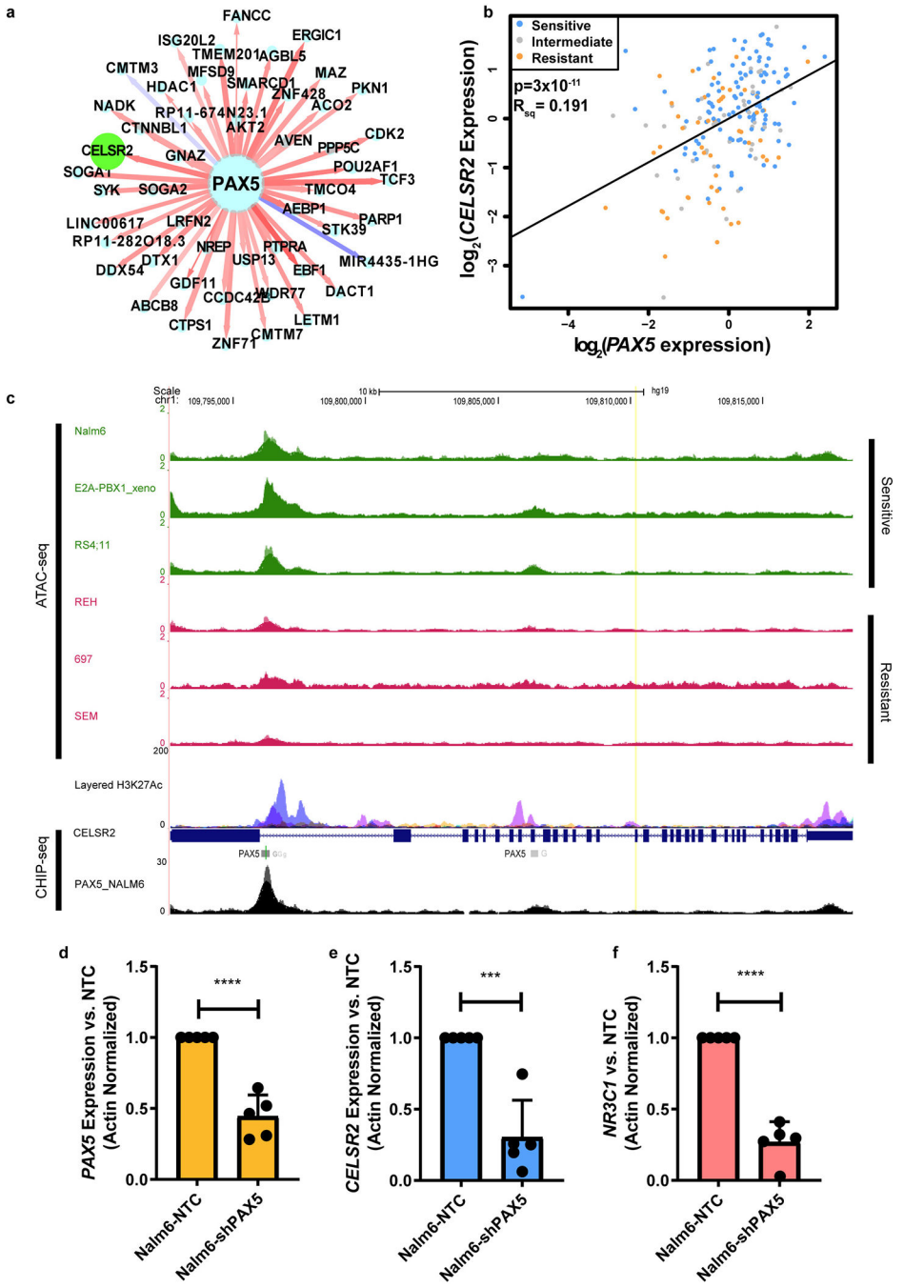

Extended Data Fig. 7. *CELSR2* mRNA expression is related to *PAX5* expression in primary ALL cells

(a.) Subnetwork (top 50 interactions ranked by mutual information) of *PAX5* and *CELSR2* from BALLi (n=185 patients). Legends of node and edge follow Figure 6c, except that nodes in green are those in top 48 drivers (Figure 6b). **(b.)** *CELSR2* expression positively correlates with *PAX5* expression in primary acute lymphoblastic leukemia cells (n= 203 patients; black line represents regression fit associated with linear model p-value and R_{sq}). *(c.)* Open chromatin regions defined by ATAC-seq (n=2 independent experiments) in three

sensitive and three resistant human leukemia cell lines and H3K27 acetylation from ENCODE in upstream 5' region of *CELSR2*. ENCODE binding site in GM12878 lymphoid cells for *PAX5* and CHIP-seq peaks from NALM-6 cells for *PAX5* binding are indicated at bottom of the plot. **(d)** *PAX5* (**** = 3.5×10^{-5}) **(e.)** *CELSR2* (*** = 3.0×10^{-4}) **(f.)** *NR3C1*(**** = 3.2×10^{-5}) protein expression (mean ± S.D.) in NALM-6 leukemia cell lines stably expressing shRNA knockdown constructs targeting *PAX5* (for d-f n=5 independent experiments; two-tailed t-test p-values).

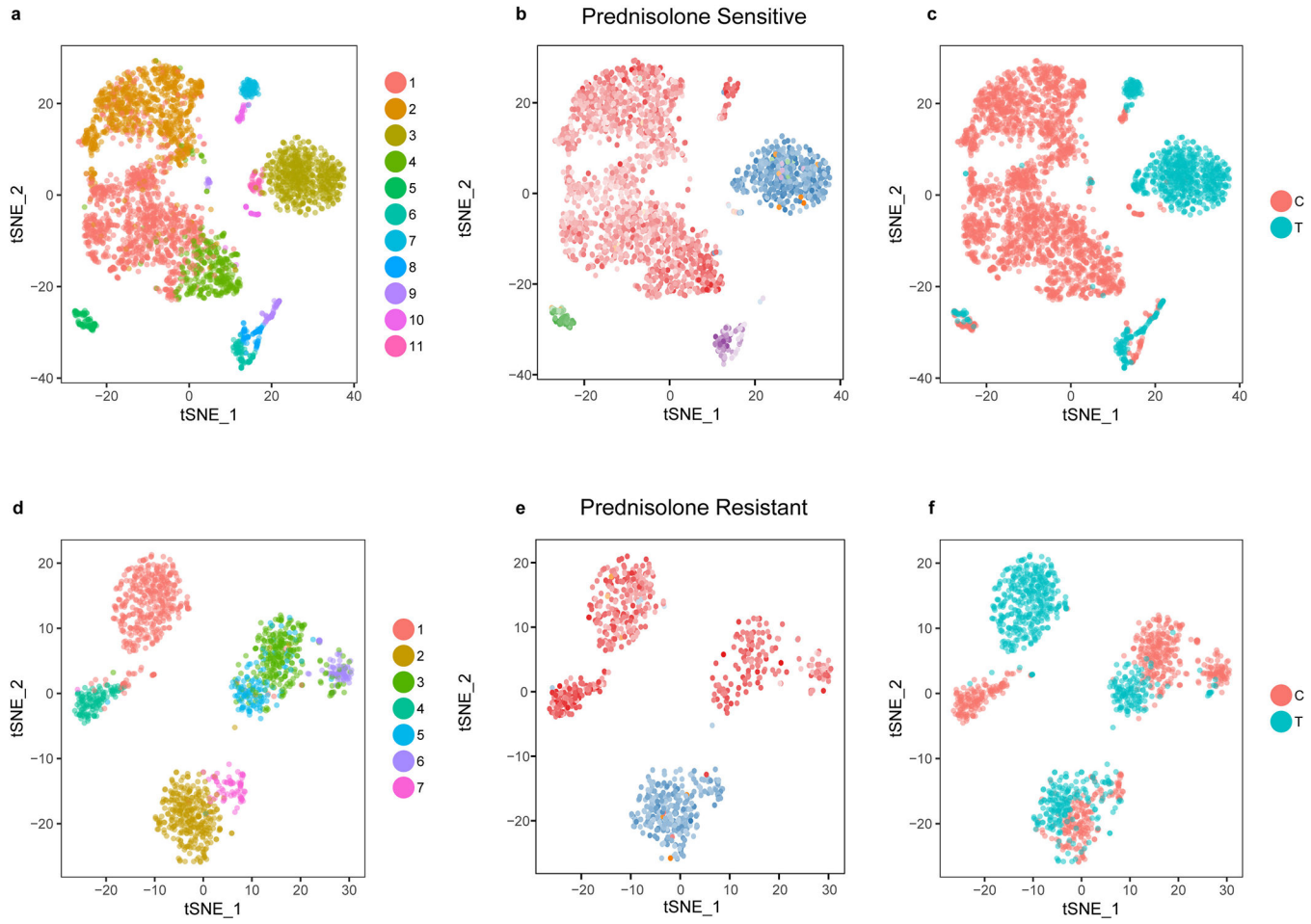

Extended Data Fig. 8. Single cell transcriptomics defines distinct expression signatures in primary B-ALL cells

(a.) Clustering of bone marrow cells from a prednisolone sensitive patient (n=2,427 control cells; n= 924 treated cells) based on top 1000 most highly expressed genes **(b.)** Identification of distinct cell populations in a prednisolone sensitive patient *CD19*+ B-cells (red), *CD3E*+ T-cells (blue), *ALAS2*+ Erythrocytes (purple) and *CD14*+ Macrophages (green) **(c.)** Control vs. treatment for all cell clusters in prednisolone sensitive patient (red = control, blue = treated) **(d.)** Clustering of bone marrow cells from a prednisolone resistant patient (n= 686 control cells; n=759 treated cells) based on top 1000 most highly expressed genes **(e.)** Identification of distinct cell populations in a prednisolone resistant patient *CD19*+ (red) and

CD3E+ T-cells (blue) **(f.)** Control (C) vs. treatment (T) for all cell clusters in prednisolone resistant patient (red = control, blue = treated)

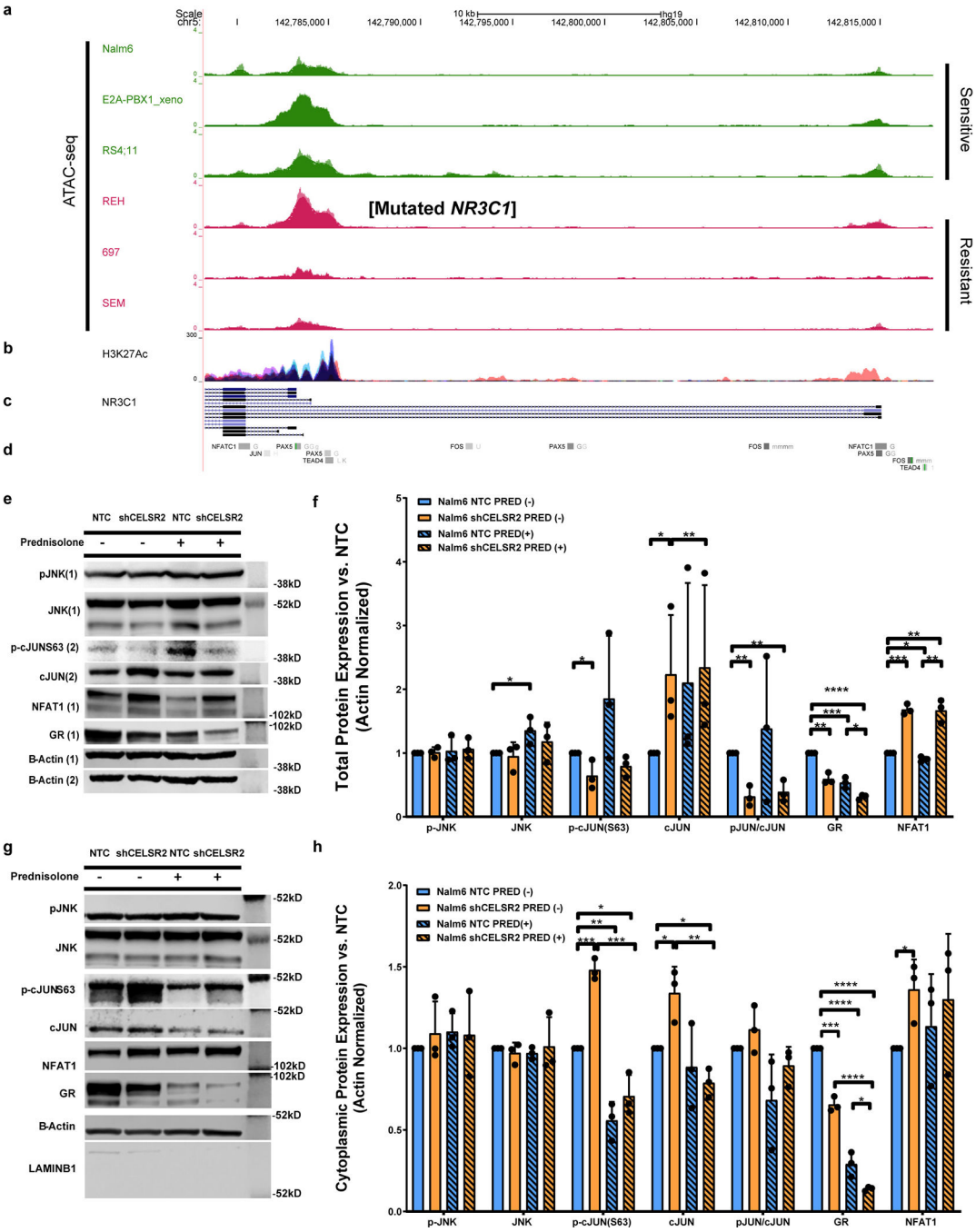

Extended Data Fig. 9. Chromatin status in glucocorticoid sensitive and resistant human ALL cell lines, and perturbation of non-canonical WNT signaling by reduction of CELSR2 expression
(a.) ATAC-seq for six human leukemia cell lines, three prednisolone sensitive and three resistant cell lines depicting open chromatin in the region upstream of *NR3C1* (n=2 independent experiments). **(b.)** H3K27Me data from ENCODE (black box) showing lymphocyte regulatory region in GM12878 cell line (pink) **(c.)** RefSeq *NR3C1* transcripts

(d.) ENCODE transcription factor binding sites for *PAX5*, *NR3C1*, *TEAD4* and non-canonical Wnt effectors (*NFATC1* and AP-1 [*JUN* and *FOS*]) **(e.)** Representative western blot and **(f.)** Barplot (mean ± S.D.; n= 3 independent experiments; two tailed t-test p values) depicting total cellular protein expression of signaling components from planar cell polarity and Ca2+/NFAT non-canonical Wnt signaling protein *CELSR2* knockdown vs. control cells with or without 10μM prednisolone treatment for 24hr. **(g.)** Representative western blot and **(h.)** Barplot (mean ± S.D.; n= 3 independent experiments; two-tailed t-test p-values) depicting cytoplasmic protein expression of signaling components from planar cell polarity and Ca2+/NFAT non-canonical Wnt signaling protein *CELSR2* knockdown vs. control cells with or without 10μM prednisolone treatment for 24hr.

Supplementary Material

Refer to Web version on PubMed Central for supplementary material.

Acknowledgements

We thank the patients and families who participated in these IRB approved studies. We also thank the technical staff in our labs (H. Williams, N. Atkinson, D. Maxwell, J. Hunt, B. Smart, Y. Wang, A. John and T. Lin), D. Bucci at Ohio State University, the Hartwell Center for Bioinformatics & Biotechnology at St. Jude Children's Research Hospital and other NCI funded Cancer Center Shared resources that supported much of the research reported herein. We would like to give special thanks to the staff of the Animal Resources Center at St. Jude Children's Research Hospital, to Dr. T. Rogers the veterinarian involved in our study, and to M. Payton for her help in our animal studies.

We would also like to thank J. Meijerink at Princess Maxima Center for advising us on previously published mechanisms of glucocorticoid resistance. Research reported in this publication was supported in part by funds from the NIH Grants R01 CA36401 (W.E.E), P50 GM115279 (M.V.R, J.J.Y, C.G.M, W.E.E.), U01 GM92666 (M.V.R, W.E.E.), St. Jude Comprehensive Cancer Center grant CA21765 from the National Cancer Institute, and by the American Lebanese Syrian Associated Charities. The content is solely the responsibility of the authors and does not necessarily represent the official views of the National Institutes of Health.

Methods Only References

1. Pieters R et al. Relation of cellular drug resistance to long-term clinical outcome in childhood acute lymphoblastic leukaemia. Lancet 338, 399–403 (1991). [PubMed: 1678081]
2. Pui CH & Evans WEA 50-year journey to cure childhood acute lymphoblastic leukemia. Semin Hematol 50, 185–196, doi:10.1053/j.seminhematol.2013.06.007 (2013). [PubMed: 23953334]
3. Pui CH & Evans WE Acute lymphoblastic leukemia. The New England journal of medicine 339, 605–615, doi:10.1056/NEJM199808273390907 (1998). [PubMed: 9718381]
4. Pui CH & Evans WE Treatment of acute lymphoblastic leukemia. The New England journal of medicine 354, 166–178, doi:10.1056/NEJMra052603 (2006). [PubMed: 16407512]
5. Clavell LA et al. Four-agent induction and intensive asparaginase therapy for treatment of childhood acute lymphoblastic leukemia. The New England journal of medicine 315, 657–663, doi:10.1056/NEJM198609113151101 (1986). [PubMed: 2943992]
6. Rhen T & Cidlowski JA Antiinflammatory action of glucocorticoids--new mechanisms for old drugs. The New England journal of medicine 353, 1711–1723, doi:10.1056/NEJMra050541 (2005). [PubMed: 16236742]
7. Dordelmann M et al. Prednisone response is the strongest predictor of treatment outcome in infant acute lymphoblastic leukemia. Blood 94, 1209–1217 (1999). [PubMed: 10438708]
8. Boer MLD et al. Patient Stratification Based on Prednisolone-Vincristine-Asparaginase Resistance Profiles in Children With Acute Lymphoblastic Leukemia. Journal of Clinical Oncology 21, 3262–3268, doi:10.1200/jco.2003.11.031 (2003). [PubMed: 12947061]

9. Kaspers GJ et al. In vitro cellular drug resistance and prognosis in newly diagnosed childhood acute lymphoblastic leukemia. Blood 90, 2723–2729 (1997). [PubMed: 9326239]
10. Schmidt S et al. Glucocorticoid-induced apoptosis and glucocorticoid resistance: molecular mechanisms and clinical relevance. Cell Death Differ 11 Suppl 1, S45–55, doi:10.1038/sj.cdd.4401456 (2004). [PubMed: 15243581]
11. Inaba H & Pui CH Glucocorticoid use in acute lymphoblastic leukaemia. The Lancet. Oncology 11, 1096–1106, doi:10.1016/S1470-2045(10)70114-5 (2010). [PubMed: 20947430]
12. Bachmann PS et al. Divergent mechanisms of glucocorticoid resistance in experimental models of pediatric acute lymphoblastic leukemia. Cancer Res 67, 4482–4490, doi:10.1158/00085472.CAN-06-4244 (2007). [PubMed: 17483364]
13. Song Q-Q, Xie W-Y, Tang Y-J, Zhang J & Liu J Genetic variation in the glucocorticoid pathway involved in interindividual differences in the glucocorticoid treatment. Pharmacogenomics 18, 293–316, doi:10.2217/pgs-2016-0151 (2017). [PubMed: 28112586]
14. Downing JR et al. The Pediatric Cancer Genome Project. Nat Genet 44, 619–622, doi:10.1038/ng.2287 (2012). [PubMed: 22641210]
15. Paugh SW et al. NALP3 inflammasome upregulation and CASP1 cleavage of the glucocorticoid receptor cause glucocorticoid resistance in leukemia cells. Nat Genet 47, 607–614, doi:10.1038/ng.3283 (2015). [PubMed: 25938942]
16. Campana D Minimal residual disease in acute lymphoblastic leukemia. Semin Hematol 46, 100–106, doi:10.1053/j.seminhematol.2008.09.001 (2009). [PubMed: 19100372]
17. Cave H et al. Clinical significance of minimal residual disease in childhood acute lymphoblastic leukemia. European Organization for Research and Treatment of Cancer--Childhood Leukemia Cooperative Group. The New England journal of medicine 339, 591–598, doi:10.1056/NEJM199808273390904 (1998). [PubMed: 9718378]
18. Pui CH et al. Clinical impact of minimal residual disease in children with different subtypes of acute lymphoblastic leukemia treated with Response-Adapted therapy. Leukemia 31, 333–339, doi:10.1038/leu.2016.234 (2017). [PubMed: 27560110]
19. Pottier N et al. The SWI/SNF chromatin-remodeling complex and glucocorticoid resistance in acute lymphoblastic leukemia. Journal of the National Cancer Institute 100, 1792–1803, doi:10.1093/jnci/djn416 (2008). [PubMed: 19066270]
20. Sanjana NE, Shalem O & Zhang F Improved vectors and genome-wide libraries for CRISPR screening. Nature methods 11, 783–784, doi:10.1038/nmeth.3047 (2014). [PubMed: 25075903]
21. Rogatsky I, Hittelman AB, Pearce D & Garabedian MJ Distinct glucocorticoid receptor transcriptional regulatory surfaces mediate the cytotoxic and cytostatic effects of glucocorticoids. Mol Cell Biol 19, 5036–5049 (1999). [PubMed: 10373553]
22. Heidari N, Miller AV, Hicks MA, Marking CB & Harada H Glucocorticoid-mediated BIM induction and apoptosis are regulated by Runx2 and c-Jun in leukemia cells. Cell Death Dis 3, e349, doi:10.1038/cddis.2012.89 (2012). [PubMed: 22825467]
23. Lochmann TL, Bouck YM & Faber AC BCL-2 inhibition is a promising therapeutic strategy for small cell lung cancer. Oncoscience 5, 218–219, doi:10.18632/oncoscience.455 (2018). [PubMed: 30234143]
24. Pham LV et al. Strategic Therapeutic Targeting to Overcome Venetoclax Resistance in Aggressive B-cell Lymphomas. Clinical Cancer Research 24, 3967, doi:10.1158/1078-0432.CCR-17-3004 (2018). [PubMed: 29666304]
25. Du X et al. Hippo/Mst signaling couples metabolic state and function of CD8α+ dendritic cells for cytotoxic T-cell priming. Nature (in press) (2018).
26. Ma X et al. Pan-cancer genome and transcriptome analyses of 1,699 paediatric leukaemias and solid tumours. Nature 555, 371–376, doi:10.1038/nature25795 (2018). [PubMed: 29489755]
27. Jing D et al. Lymphocyte-Specific Chromatin Accessibility Pre-determines Glucocorticoid Resistance in Acute Lymphoblastic Leukemia. Cancer Cell 34, 906–921 e908, doi:10.1016/j.ccell.2018.11.002 (2018). [PubMed: 30537513]
28. Jing D et al. Opposing regulation of BIM and BCL2 controls glucocorticoid-induced apoptosis of pediatric acute lymphoblastic leukemia cells. Blood 125, 273–283, doi:10.1182/blood-2014-05-576470 (2015). [PubMed: 25336632]

29. Consortium EP An integrated encyclopedia of DNA elements in the human genome. Nature 489, 57–74, doi:10.1038/nature11247 (2012). [PubMed: 22955616]
30. Sugimura R et al. Noncanonical Wnt signaling maintains hematopoietic stem cells in the niche. Cell 150, 351–365, doi:10.1016/j.cell.2012.05.041 (2012). [PubMed: 22817897]
31. Presul E, Schmidt S, Kofler R & Helmberg A Identification, tissue expression, and glucocorticoid responsiveness of alternative first exons of the human glucocorticoid receptor. J Mol Endocrinol 38, 79–90, doi:10.1677/jme.1.02183 (2007). [PubMed: 17242171]
32. Pui CH, Ochs J, Kalwinsky DK & Costlow ME Impact of treatment efficacy on the prognostic value of glucocorticoid receptor levels in childhood acute lymphoblastic leukemia. Leuk Res 8, 345–350 (1984). [PubMed: 6379308]
33. Irving JA, Minto L, Bailey S & Hall AG Loss of heterozygosity and somatic mutations of the glucocorticoid receptor gene are rarely found at relapse in pediatric acute lymphoblastic leukemia but may occur in a subpopulation early in the disease course. Cancer Res 65, 9712–9718, doi:10.1158/0008-5472.CAN-05-1227 (2005). [PubMed: 16266991]
34. Tremblay CS et al. Loss-of-function mutations of Dynamin 2 promote T-ALL by enhancing IL-7 signalling. Leukemia 30, 1993–2001, doi:10.1038/leu.2016.100 (2016). [PubMed: 27118408]
35. Li Y et al. IL-7 Receptor Mutations and Steroid Resistance in Pediatric T cell Acute Lymphoblastic Leukemia: A Genome Sequencing Study. PLoS medicine 13, e1002200, doi:10.1371/journal.pmed.1002200 (2016). [PubMed: 27997540]
36. Delgado-Martin C et al. JAK/STAT pathway inhibition overcomes IL7-induced glucocorticoid resistance in a subset of human T-cell acute lymphoblastic leukemias. Leukemia 31, 2568–2576, doi:10.1038/leu.2017.136 (2017). [PubMed: 28484265]
37. Oppermann S et al. Janus and PI3-kinases mediate glucocorticoid resistance in activated chronic leukemia cells. Oncotarget 7, 72608–72621, doi:10.18632/oncotarget.11618 (2016). [PubMed: 27579615]
38. Kruth KA et al. Suppression of B-cell development genes is key to glucocorticoid efficacy in treatment of acute lymphoblastic leukemia. Blood 129, 3000–3008, doi:10.1182/blood-2017-02-766204 (2017). [PubMed: 28424165]
39. Wei G et al. Gene expression-based chemical genomics identifies rapamycin as a modulator of MCL1 and glucocorticoid resistance. Cancer Cell 10, 331–342, doi:10.1016/j.ccr.2006.09.006 (2006). [PubMed: 17010674]
40. Bonapace L et al. Induction of autophagy-dependent necroptosis is required for childhood acute lymphoblastic leukemia cells to overcome glucocorticoid resistance. J Clin Invest 120, 1310–1323, doi:10.1172/JCI39987 (2010). [PubMed: 20200450]
41. Piovan E et al. Direct reversal of glucocorticoid resistance by AKT inhibition in acute lymphoblastic leukemia. Cancer Cell 24, 766–776, doi:10.1016/j.ccr.2013.10.022 (2013). [PubMed: 24291004]
42. Nicholson L et al. Quantitative proteomic analysis reveals maturation as a mechanism underlying glucocorticoid resistance in B lineage ALL and re-sensitization by JNK inhibition. British journal of haematology 171, 595–605, doi:10.1111/bjh.13647 (2015). [PubMed: 26310606]
43. Chan LN et al. Metabolic gatekeeper function of B-lymphoid transcription factors. Nature 542, 479–483, doi:10.1038/nature21076 (2017). [PubMed: 28192788]
44. Jones CL et al. Loss of TBL1XR1 disrupts glucocorticoid receptor recruitment to chromatin and results in glucocorticoid resistance in a B-lymphoblastic leukemia model. J Biol Chem 289, 20502–20515, doi:10.1074/jbc.M114.569889 (2014). [PubMed: 24895125]
45. Jones CL et al. MAPK signaling cascades mediate distinct glucocorticoid resistance mechanisms in pediatric leukemia. Blood 126, 2202–2212, doi:10.1182/blood-2015-04-639138 (2015). [PubMed: 26324703]
46. Hosono N et al. Glutathione S-transferase M1 inhibits dexamethasone-induced apoptosis in association with the suppression of Bim through dual mechanisms in a lymphoblastic leukemia cell line. Cancer Sci 101, 767–773, doi:10.1111/j.1349-7006.2009.01432.x (2010). [PubMed: 20067466]

47. Kotani A et al. miR-128b is a potent glucocorticoid sensitizer in MLL-AF4 acute lymphocytic leukemia cells and exerts cooperative effects with miR-221. Blood 114, 4169–4178, doi:10.1182/blood-2008-12-191619 (2009). [PubMed: 19749093]
48. Han BW et al. A set of miRNAs that involve in the pathways of drug resistance and leukemic stem-cell differentiation is associated with the risk of relapse and glucocorticoid response in childhood ALL. Hum Mol Genet 20, 4903–4915, doi:10.1093/hmg/ddr428 (2011). [PubMed: 21926415]
49. Zhao JJ et al. Targeting the miR-221–222/PUMA/BAK/BAX Pathway Abrogates Dexamethasone Resistance in Multiple Myeloma. Cancer Res 75, 4384–4397, doi:10.1158/0008-5472.CAN-15-0457 (2015). [PubMed: 26249174]
50. Spijkers-Hagelstein JA, Mimoso Pinhancos S, Schneider P, Pieters R & Stam RW Src kinase-induced phosphorylation of annexin A2 mediates glucocorticoid resistance in MLL-rearranged infant acute lymphoblastic leukemia. Leukemia 27, 1063–1071, doi:10.1038/leu.2012.372 (2013). [PubMed: 23334362]
51. Spijkers-Hagelstein JA et al. Elevated S100A8/S100A9 expression causes glucocorticoid resistance in MLL-rearranged infant acute lymphoblastic leukemia. Leukemia 26, 1255–1265, doi:10.1038/leu.2011.388 (2012). [PubMed: 22282267]
52. Aries IM et al. EMP1, a novel poor prognostic factor in pediatric leukemia regulates prednisolone resistance, cell proliferation, migration and adhesion. Leukemia 28, 1828–1837, doi:10.1038/leu.2014.80 (2014). [PubMed: 24625531]
53. Yang JJ et al. Genome-wide association study identifies germline polymorphisms associated with relapse of childhood acute lymphoblastic leukemia. Blood 120, 4197–4204, doi:10.1182/blood-2012-07-440107 (2012). [PubMed: 23007406]
54. Meyers JA, Taverna J, Chaves J, Makkinje A & Lerner A Phosphodiesterase 4 inhibitors augment levels of glucocorticoid receptor in B cell chronic lymphocytic leukemia but not in normal circulating hematopoietic cells. Clin Cancer Res 13, 4920–4927, doi:10.1158/1078-0432.CCR-07-0276 (2007). [PubMed: 17699872]
55. Zhou M et al. Targeting of the deubiquitinase USP9X attenuates B-cell acute lymphoblastic leukemia cell survival and overcomes glucocorticoid resistance. Biochemical and Biophysical Research Communications 459, 333–339, doi:10.1016/j.bbrc.2015.02.115 (2015). [PubMed: 25735983]
56. Rocha JC et al. Pharmacogenetics of outcome in children with acute lymphoblastic leukemia. Blood 105, 4752–4758, doi:10.1182/blood-2004-11-4544 (2005). [PubMed: 15713801]
57. Mullighan CG et al. CREBBP mutations in relapsed acute lymphoblastic leukaemia. Nature 471, 235–239, doi:10.1038/nature09727 (2011). [PubMed: 21390130]
58. Malyukova A et al. FBXW7 regulates glucocorticoid response in T-cell acute lymphoblastic leukaemia by targeting the glucocorticoid receptor for degradation. Leukemia 27, 1053–1062, doi:10.1038/leu.2012.361 (2013). [PubMed: 23228967]
59. Park HW et al. Alternative Wnt Signaling Activates YAP/TAZ. Cell 162, 780–794, doi:10.1016/j.cell.2015.07.013 (2015). [PubMed: 26276632]
60. Cortijo C, Gouzi M, Tissir F & Grapin-Botton A Planar cell polarity controls pancreatic beta cell differentiation and glucose homeostasis. Cell reports 2, 1593–1606, doi:10.1016/j.celrep.2012.10.016 (2012). [PubMed: 23177622]
61. Cabral AL, Hays AN, Housley PR, Brentani MM & Martins VR Repression of glucocorticoid receptor gene transcription by c-Jun. Mol Cell Endocrinol 175, 67–79 (2001). [PubMed: 11325517]
62. Holleman A et al. Gene-expression patterns in drug-resistant acute lymphoblastic leukemia cells and response to treatment. The New England journal of medicine 351, 533–542, doi:10.1056/NEJMoa033513 (2004). [PubMed: 15295046]
63. Coustan-Smith E et al. New markers for minimal residual disease detection in acute lymphoblastic leukemia. Blood 117, 6267–6276, doi:10.1182/blood-2010-12-324004 (2011). [PubMed: 21487112]
64. Cheok MH et al. Treatment-specific changes in gene expression discriminate in vivo drug response in human leukemia cells. Nat Genet 34, 85–90, doi:10.1038/ng1151 (2003). [PubMed: 12704389]

65. Yeoh EJ et al. Classification, subtype discovery, and prediction of outcome in pediatric acute lymphoblastic leukemia by gene expression profiling. Cancer Cell 1, 133–143 (2002). [PubMed: 12086872]

66. Kuan PF, Wang S, Zhou X & Chu H A statistical framework for Illumina DNA methylation arrays. Bioinformatics 26, 2849–2855, doi:10.1093/bioinformatics/btq553 (2010). [PubMed: 20880956]

67. French D et al. Acquired variation outweighs inherited variation in whole genome analysis of methotrexate polyglutamate accumulation in leukemia. Blood 113, 4512–4520, doi:10.1182/blood-2008-07-172106 (2009). [PubMed: 19066393]

68. Paugh SW et al. MicroRNAs Form Triplexes with Double Stranded DNA at Sequence-Specific Binding Sites; a Eukaryotic Mechanism via which microRNAs Could Directly Alter Gene Expression. PLoS Comput Biol 12, e1004744, doi:10.1371/journal.pcbi.1004744 (2016). [PubMed: 26844769]

69. Zhang J et al. The genetic basis of early T-cell precursor acute lymphoblastic leukaemia. Nature 481, 157–163, doi:10.1038/nature10725 (2012). [PubMed: 22237106]

70. Liu Y et al. The genomic landscape of pediatric and young adult T-lineage acute lymphoblastic leukemia. Nature Genetics 49, 1211, doi:10.1038/ng.3909 (2017). [PubMed: 28671688]

71. Shalem O et al. Genome-scale CRISPR-Cas9 knockout screening in human cells. Science 343, 84–87, doi:10.1126/science.1247005 (2014). [PubMed: 24336571]

72. Li W et al. MAGeCK enables robust identification of essential genes from genome-scale CRISPR/Cas9 knockout screens. Genome Biol 15, 554, doi:10.1186/s13059-014-0554-4 (2014). [PubMed: 25476604]

73. Li W et al. Quality control, modeling, and visualization of CRISPR screens with MAGeCK-VISPR. Genome Biol 16, 281, doi:10.1186/s13059-015-0843-6 (2015). [PubMed: 26673418]

74. Cheng C & Parzen E Unified estimators of smooth quantile and quantile density functions. Journal of Statistical Planning and Inference 59, 291–307, doi:10.1016/S0378-3758(96)00110-3 (1997).

75. De Vore RA The approximation of continuous functions by positive linear operators. (Springer-Verlag, 1972).

76. Cheng C in Optimality Vol. Number 49 Lecture Notes--Monograph Series (ed Rojo Javier) 51–76 (Institute of Mathematical Statistics, 2006).

77. Maaten L v. d. Accelerating t-SNE using Tree-Based Algorithms. Journal of Machine Learning Research 115, 3221–3245 (2014).

78. Macosko EZ et al. Highly Parallel Genome-wide Expression Profiling of Individual Cells Using Nanoliter Droplets. Cell 161, 1202–1214, doi:10.1016/j.cell.2015.05.002 (2015). [PubMed: 26000488]

79. Ward JH Hierarchical Grouping to Optimize an Objective Function. Journal of the American Statistical Association 58, 236–244, doi:10.1080/01621459.1963.10500845 (1963).

80. Savic D et al. Distinct gene regulatory programs define the inhibitory effects of liver X receptors and PPARG on cancer cell proliferation. Genome Med 8, 74, doi:10.1186/s13073-016-0328-6 (2016). [PubMed: 27401066]

81. Corces MR et al. Lineage-specific and single-cell chromatin accessibility charts human hematopoiesis and leukemia evolution. Nat Genet 48, 1193–1203, doi:10.1038/ng.3646 (2016). [PubMed: 27526324]

82. Du X et al. Hippo/Mst signaling couples metabolic state and function of CD8α+ dendritic cells for cytotoxic T-cell priming. Nature (accepted) (2018).

83. Khaw SL et al. Venetoclax responses of pediatric ALL xenografts reveal sensitivity of MLL-rearranged leukemia. Blood 128, 1382–1395, doi:10.1182/blood-2016-03-707414 (2016). [PubMed: 27343252]

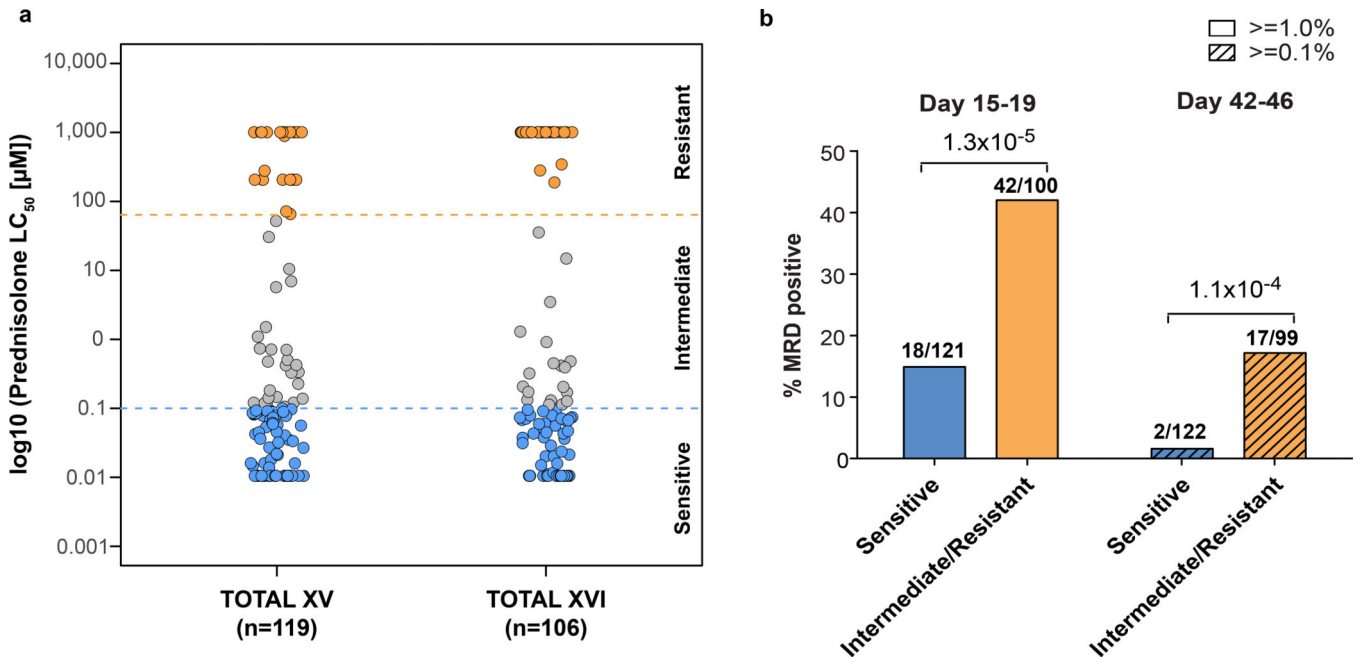

Figure 1. *De novo* sensitivity of primary leukemia cells to prednisolone and clinical treatment response

a) Distribution of prednisolone LC_{50} values in the discovery cohort, comprising children with acute lymphoblastic leukemia enrolled on two consecutive research protocols at St. Jude (n=119 and n =106 ALL patients, respectively) depicting >10,000- fold range in *ex vivo* sensitivity. Horizontal dashed lines depict LC_{50} values discriminating prednisolone sensitive, intermediate and resistant cases using previously reported values.[15] **b)** The percentage of patients who had minimal residual disease (MRD) in their bone marrow at day 15–19 of treatment (MRD ≥ 1%) or at day 42–46 of treatment (MRD ≥0.1%) differed significantly based on prednisolone sensitivity (Chi-Square test p-value; n=221 ALL patients).

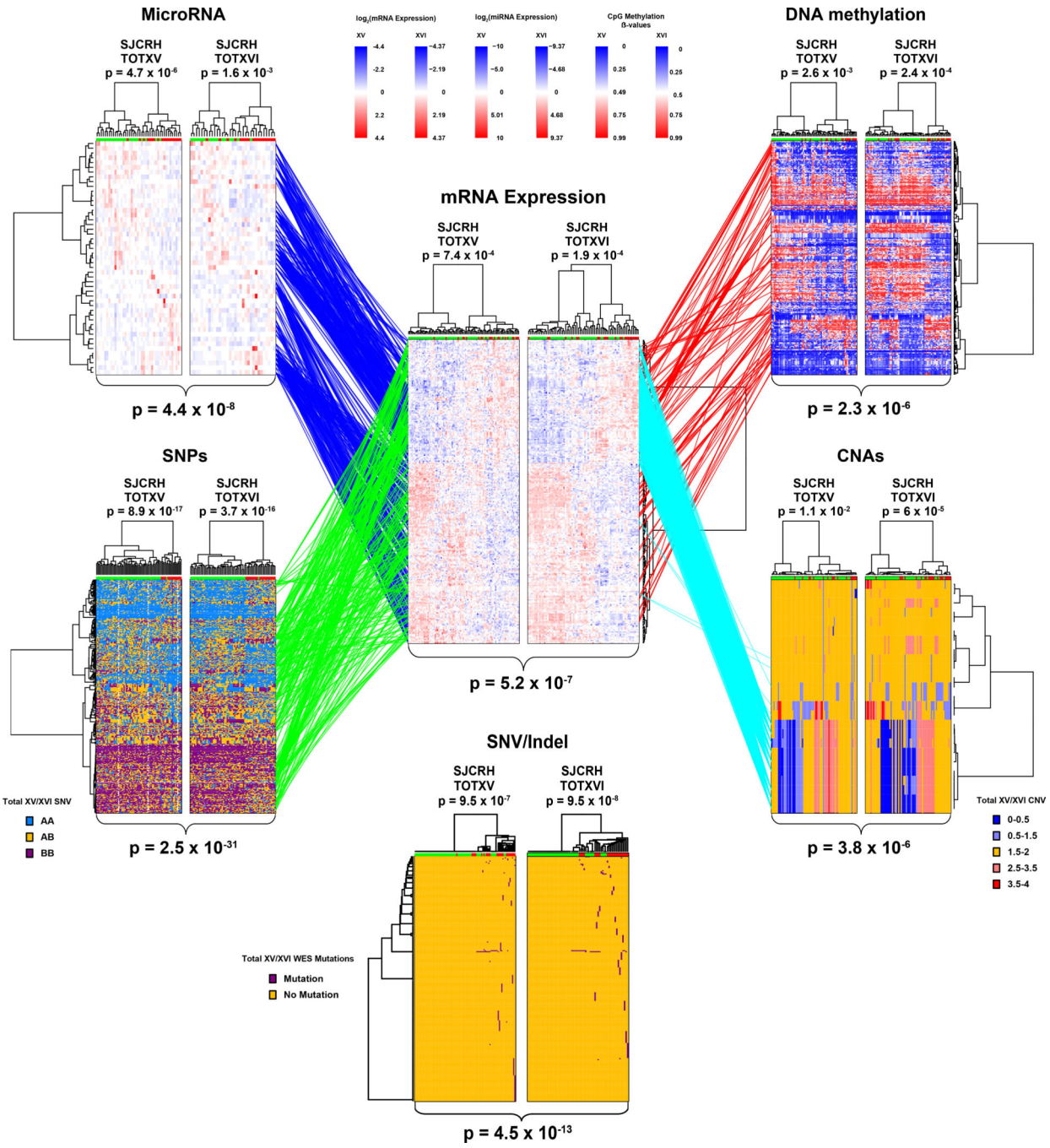

Figure 2: Polygenomic analyses identify genomic features related to prednisolone resistance

Leukemia cell mRNA, miRNA, DNA methylation, copy number alterations (CNAs), single nucleotide polymorphisms (SNPs) or coding SNVs/Indels (by WES) that significantly discriminate prednisolone sensitive and resistant ALL, by hierarchical clustering in the discovery cohorts (TOTXV and TOTXVI). Each column represents an individual patient's ALL cells, those labeled at the top with green are sensitive and those with red are resistant to prednisolone; each row indicates a different probe. (Center panel) mRNA expression vs prednisolone LC_{50}: heat map depicts high (red) or low (blue) gene expression relative to the

mean signal for that probe set in the entire cohort [n=254 mRNA probes; n= 203 patients]. (Top left) heat map for miRNA expression versus LC_{50}; red and blue denote higher versus lower expression relative to mean signal for probe amongst the entire cohort [n=49 miRNAs; n=163 patients]. (Top Right) DNA methylation versus $LC_{50;}$ red and blue denote higher versus lower methylation signal [n=203 CpG probes; n=178 patients] (Bottom left) single nucleotide polymorphisms (SNPs) associated with LC_{50} blue = AA, orange = AB, purple = BB [n=380 SNPs; n=184 patients]. (Bottom right) copy number alterations (CNAs) associated with LC_{50}; red = copy gain, blue = copy loss, orange = copy neutral [n=25 CNAs; n= 184 patients]. (Bottom center) SNVs and Indels by WES [n=227 SNVs/Indels] associated with LC_{50}; purple = mutation, orange = non-mutated. (Lines) lines connecting probe sets are drawn where significant associations were found between mRNA expression levels and a specific peripheral genomic feature. DNA methylation and miRNA connections were required to be significantly negatively associated with mRNA expression; DNA methylation probes were also required to be within 100kb of the gene encoding the mRNA and miRNAs were required to have a predicted binding site in the gene and/or experimental evidence from literature. Connections between SNVs/Indels and mRNA are provided in Extended Data Fig. 2d. P-values for each heatmap (at top) indicate the results of Fisher's exact tests comparing the distribution of sensitive and resistant cases when the highest level of the dendrogram is split in two. Overall clustering P-values for each heatmap (at bottom) are the result of Stouffer's meta-analysis of corresponding individual Fisher's exact test (two-sided) p-values within each cohort.

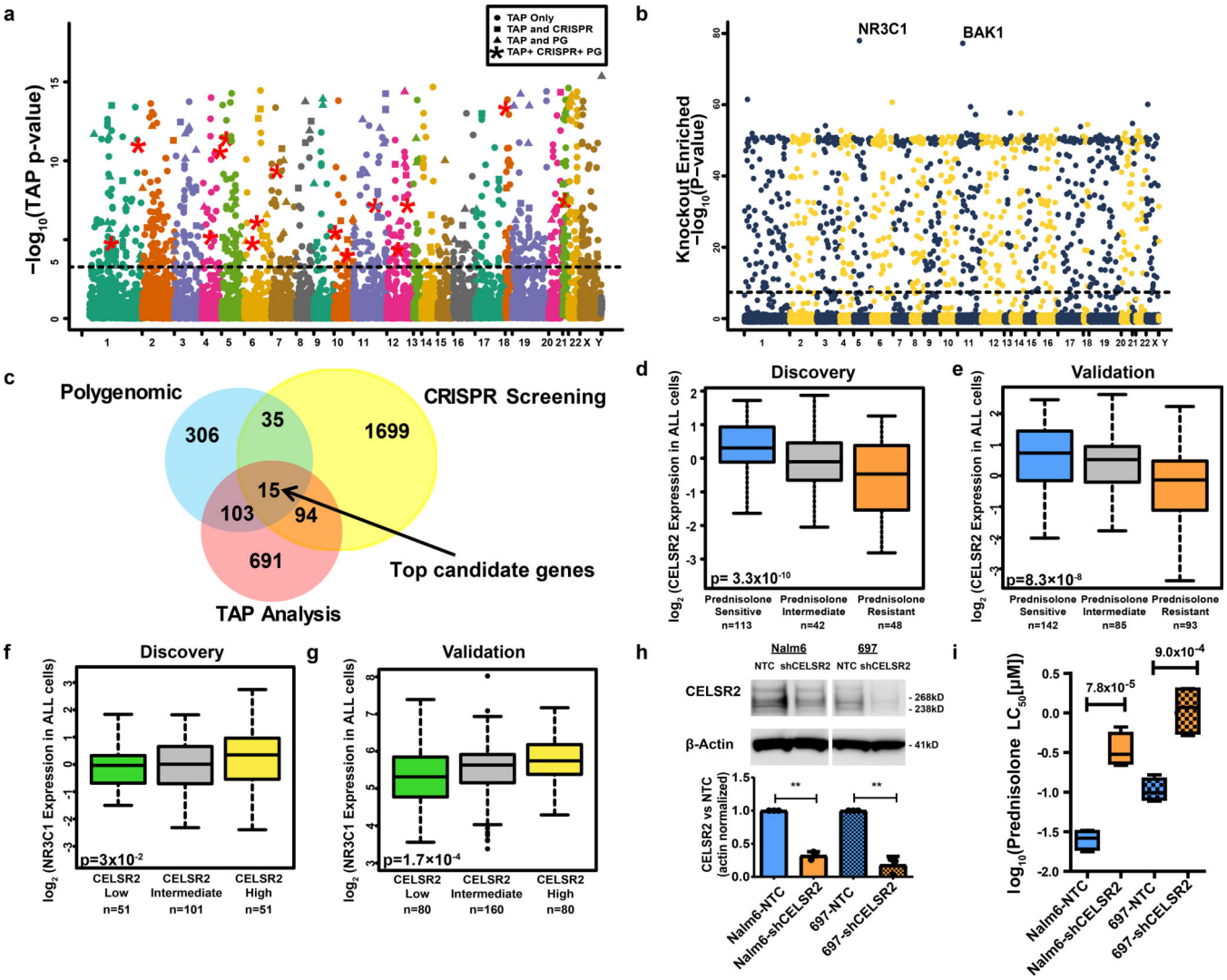

Figure 3. Genomewide orthogonal validation identifies *CELSR2* as a key mediator of glucocorticoid resistance

(a.) Manhattan plot of gene-level aggregated p-values (TAP statistic) for all 19,725 genes (n= 203 patients) (illustrated in regional plots for four genes in Extended Data Fig. 5). Circles above the blue dotted threshold line represent genes only significant in TAP analysis, squares depict genes significant in both the TAP and CRISPR screen, triangles represent genes significant in both the polygenomic analysis and the TAP analysis, and red stars depict the 15 genes significant in all three analyses (linear regression p-value cutoff [adjusted for massive multiple testing by adaptive thresholding] = 5.38×10^{-4}). **(b.)** −log10 p-values for genes (n=19,050 genes in two replicate experiments) interrogated in the CRISPR knockout screen ("knockout enriched"). The threshold for statistical significance (logit gene-level one-sided p= 4.0×10^{-8} [FDR adjusted p = 5.2×10^{-7}]) of association with prednisolone resistance is depicted by the horizontal dotted line. **(c.)** Venn diagram showing overlap among genes significant in each analysis with 15 genes significant in all three analyses. **(d-e)** *CELSR2* mRNA expression in leukemia cells from newly diagnosed patients enrolled on St. Jude clinical trials, grouped based on prednisolone sensitivity (LC_{50}) in **(d.)** the discovery cohort

(n=203; linear model p-value) and **(e.)** an independent validation cohort (n=320 patients; linear model p-value). **(f-g)** *NR3C1* mRNA expression in leukemia cells from newly diagnosed patients enrolled on two St. Jude clinical trials, grouped based on *CELSR2* expression (low ≤ lower quartile, high ≥ upper quartile and intermediate falls between the upper and lower quartile of *CELSR2* expression) in **(f.)** the discovery cohort (n=203 patients; linear model p-value) and **(g.)** an independent validation cohort (n=320 patients; linear model p-value). **(h.)** Representative western blot and bar graph quantifying n=3 biologically independent experiments of *CELSR2* knockdown (mean ± SD) in two human B-lineage leukemia cell lines (NALM-6 two tailed t-test p-value = 0.0026 and 697 two-tailed p-value = 0.0081; ** = <0.01; cropping performed uncropped image available as source data). **(i.)** Prednisolone LC_{50} values in human ALL cells lines (NALM-6 and 697) expressing *CELSR2* shRNA (~70% knockdown) or non-target control (n=4 independent experiments; two-tailed t-test p-value) For all boxplots, horizontal bars depict medians and boxes represent 25^{th} and 75^{th} percentiles, whiskers represent ±1.5x interquartile range (IQR); p-values are two-tailed t-test.

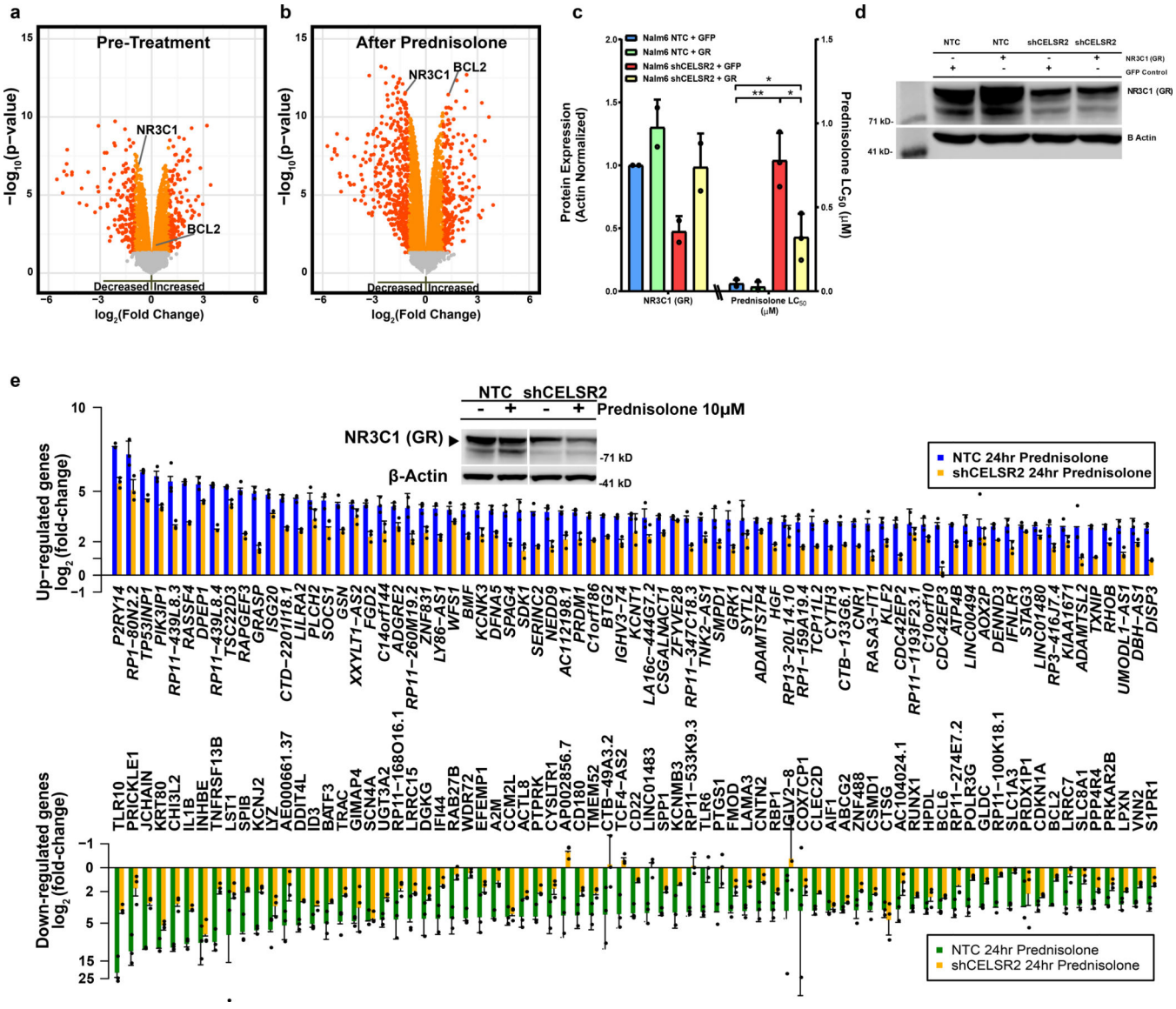

Figure 4. *CELSR2* knockdown decreases GR expression and attenuates glucocorticoid modulation of gene expression

(a.) Volcano plot (n= 3 independent experiments) for untreated *CELSR2* knockdown human leukemia cell line (NALM-6) vs. non-target control (NTC). Left side of plot depicts genes with reduced expression in *CELSR2* knockdown cells and genes to the right exhibiting increased expression in *CELSR2* knockdown cells. Orange and red symbols depict mRNAs with significant changes in expression (linear model p-value); red symbols have a fold change greater than 2. **(b.)** Volcano plot of gene expression after 24 hours of 10μM prednisolone treatment of *CELSR2* knockdown vs. non-target control ALL cells (NALM-6, n=3 independent experiments; linear model p-value). **(c.)** (left) NR3C1 protein quantification (n= 2 independent experiments) or (right) Prednisolone LC_{50} (n=3 independent experiments; mean ± SD) in NALM-6 NTC or shCELSR2 cells with either GFP control or re-introduction of *NR3C1* (two tailed t-test p-value; * =p < 0.05, ** = p <0.01, *** = p <0.001). **(d.)** Representative western blot of GR protein expression (n= 2

independent experiments) in NTC or shCELSR2 NALM-6 cells with or without GR re-expression. **(e.)** The 75 most highly upregulated (top) or downregulated (bottom) genes in human NALM-6 ALL cells after 24 hours treatment with 10μM prednisolone (n= 3 independent experiments). Blue and green bars depict mRNA expression in NALM-6 cells transfected with non-target control vector and gold bars depict blunted induction or repression in cells expressing shRNA for *CELSR2* knockdown (mean ± SD). (Inset) Representative western blot (n= 3 independent experiments) showing significantly lower GR levels in *CELSR2* knockdown cell lines compared to non-targeting controls, with or without prednisolone treatment for 24hr (cropping performed uncropped image available as source data).

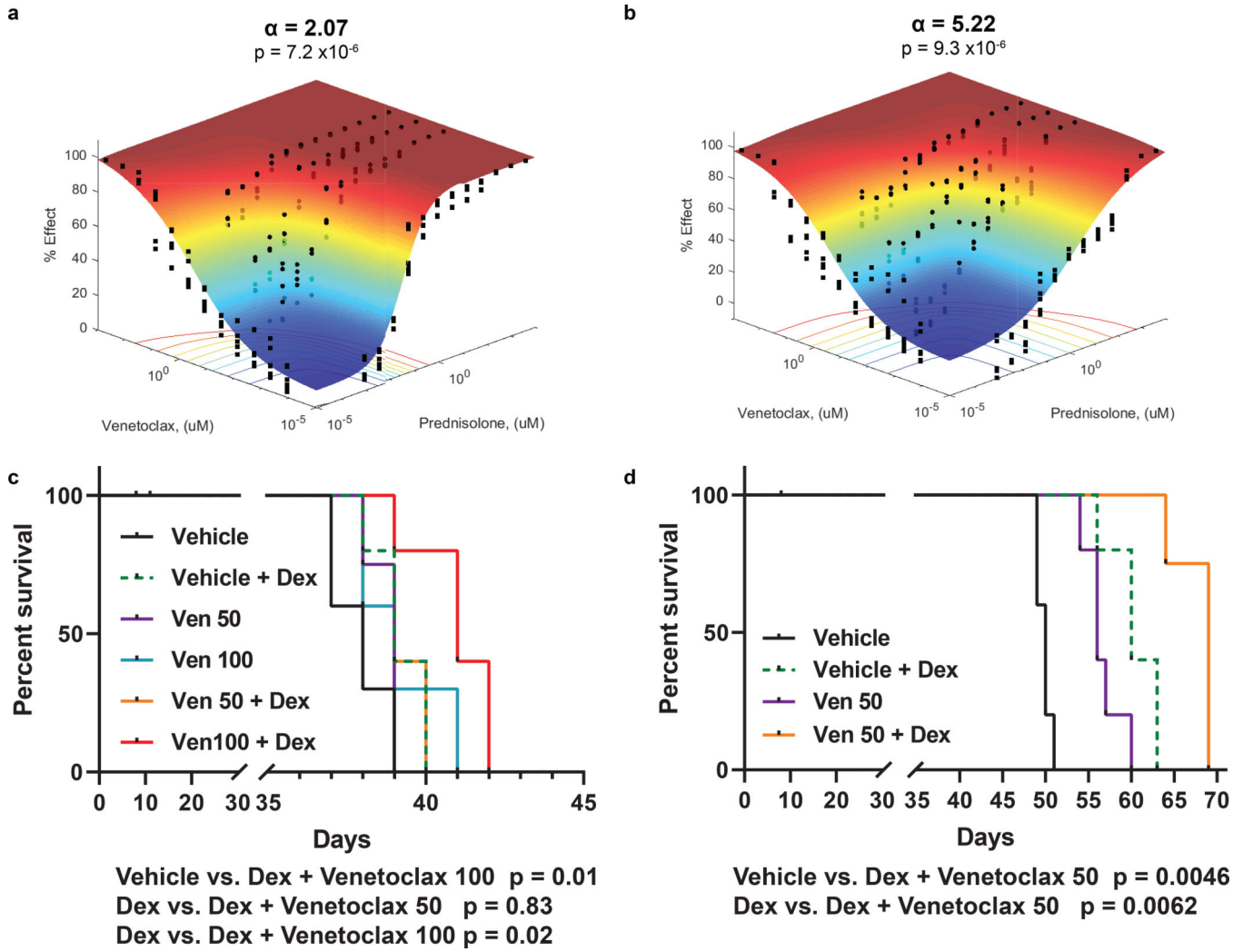

Figure 5. Increased synergy and mitigation of glucocorticoid resistance by inhibition of *BCL2* in ALL with low *CELSR2* expression

(a.) Response surface model (% Effect = % cell kill) depicting synergy between prednisolone and Bcl-2 inhibitor venetoclax in NALM-6 cells transduced with non-target control or **(b.)** *CELSR2* knockdown ALL cells (n= 3 independent experiments; response surface model two-tailed t-test p-value). The (α) value indicates antagonism < 0 or synergy > 0, with higher values representing greater synergy. P-value assesses overall model fit. **(c.)** Percent survival of NSG mice inoculated with 100,000 NALM-6 non-target control cells or **(d.)** 100,000 *CELSR2* knockdown leukemia cells treated with either vehicle, dexamethasone alone (4 mg/kg), venetoclax alone (50 or 100 mg/kg) or combination of venetoclax with dexamethasone (n= 5 mice per treatment group; Log-rank (Mantel-Cox) test p-values).

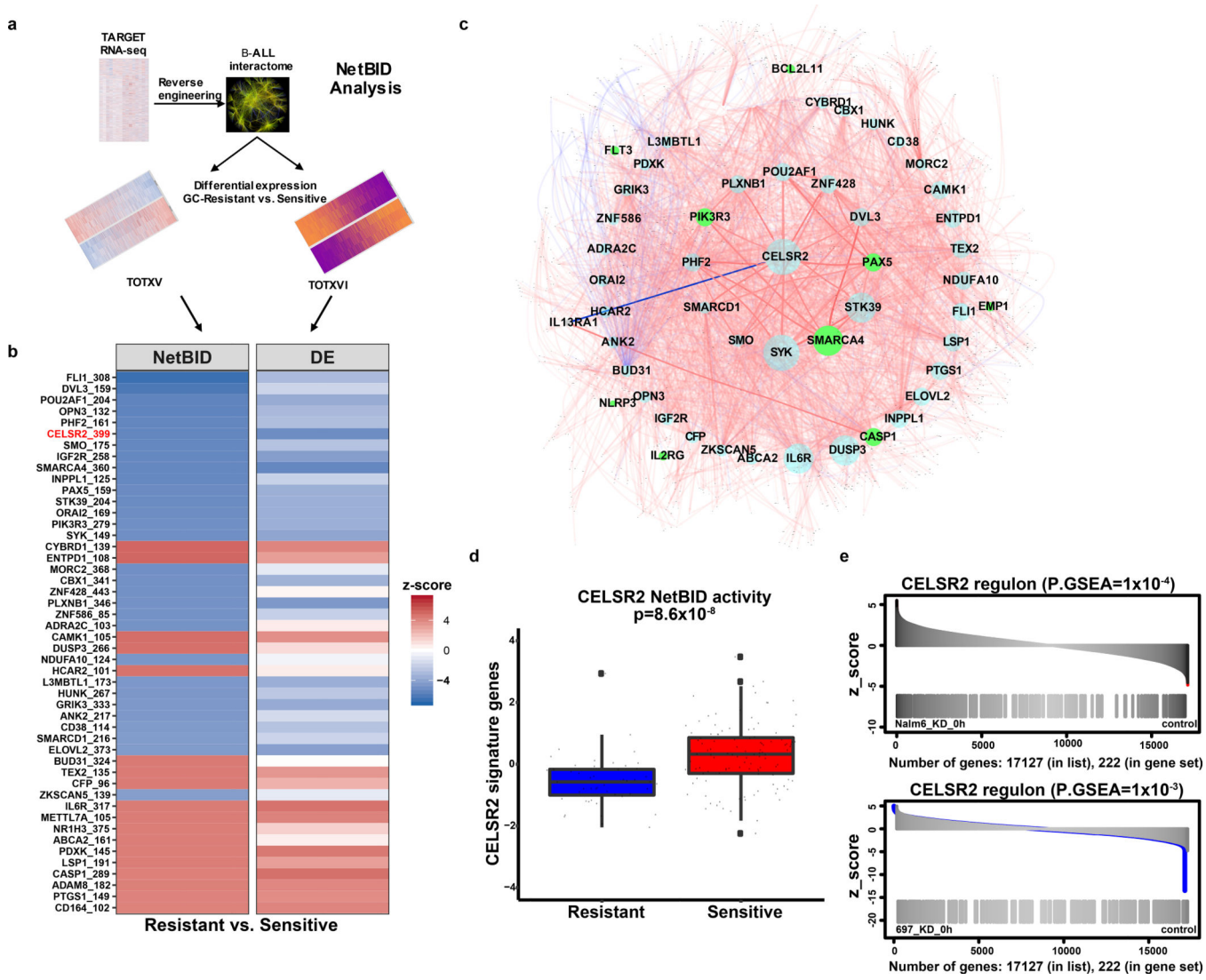

Figure 6. NetBID identifies *CELSR2* as a hub driver of prednisolone resistance

(a.) Schematic workflow representing NetBID algorithm **(b.)** Heatmap of top 48 NetBID-predicted drivers from total of n=7,920 drivers inferred from the B-ALL interactome (n=185 patients) that were associated with prednisolone resistance (n=203 patients with gene expression and LC_{50}). Drivers (as denoted by "symbol_regulon size", e.g. "*CELSR2_399*") are ranked by integrated NetBID p-value. (Left) Combined NetBID results color-coded by z-score (red = positive, blue = negative); Right: differential expression (DE) of each driver itself, color-coded by z-score. **(c.)** Subnetwork of the top 48 drivers versus prednisolone LC_{50} in relation to one another (limited to top 50 interactions for each driver ranked by mutual information of each hub gene) from B-ALLi. Node size is proportional to the regulon size; nodes in green represent known resistance genes. Edges: width is proportional to mutual information, red is for positive and blue for negative Spearman correlations of the connecting nodes. **(d.)** *CELSR2* NetBID activities (horizontal bar depicts median and boxes represent 25th and 75th percentiles, whiskers represent ±1.5x IQR) in prednisolone resistant and sensitive patients from TOTXV and TOTXVI patient cohorts (Stouffer's combined

Bayesian generalized linear model “NetBID” p-value; n=203 patients). **(e.)** Enrichment of NetBID-inferred *CELSR2* regulon (n= 399 genes) in differentially expressed genes (n= 222 genes) of *CELSR2* knockdown vs. control in NALM-6 (top) and 697 (bottom) cell lines without prednisolone treatment.

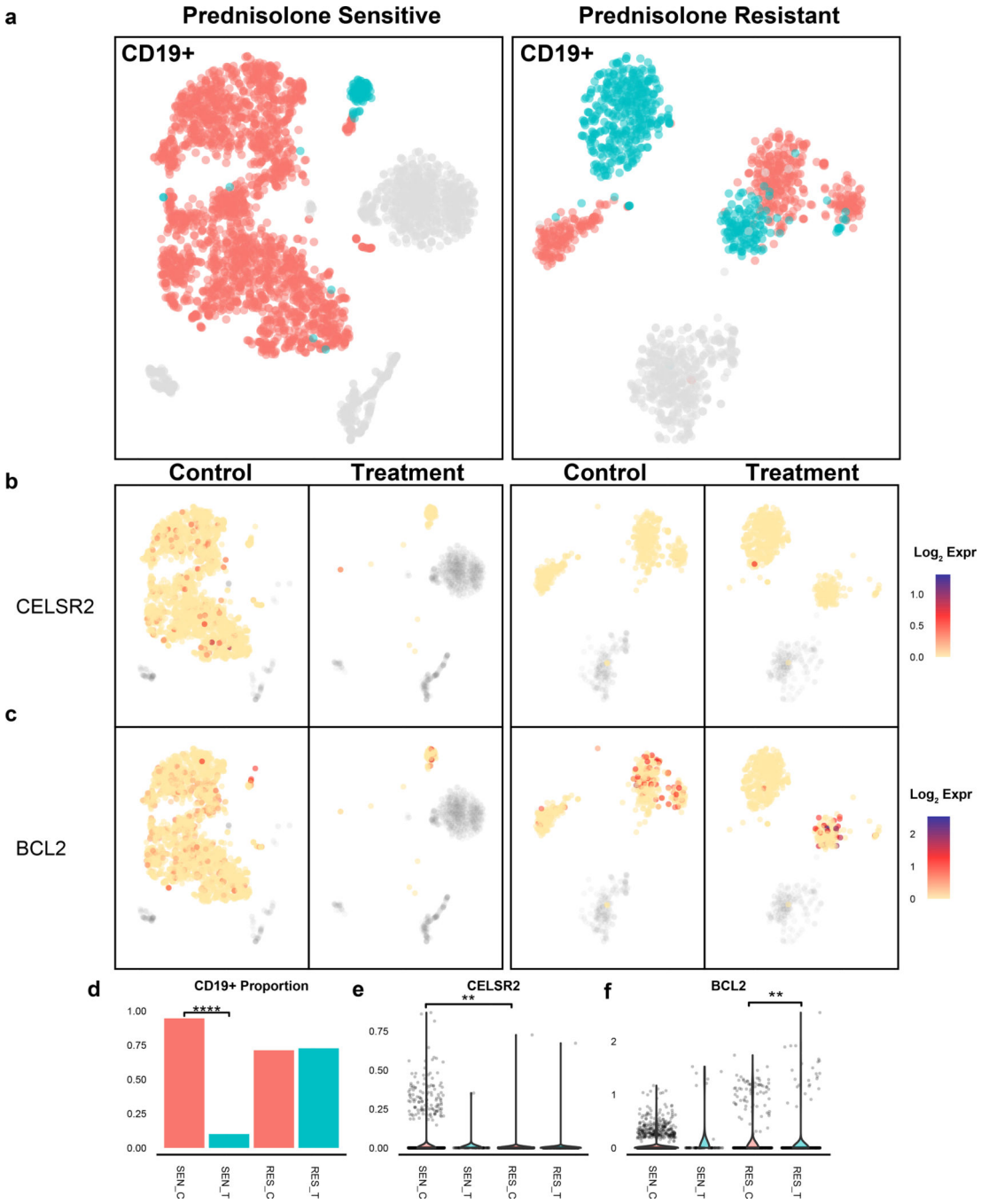

Figure 7. Single cell transcriptomic analysis verifies lower *CELSR2* and higher *BCL2* in glucocorticoid-resistant primary ALL cells

(a.) Clustering of single cells (n= 2 patients) based upon the top 1000 most highly expressed genes. Both patients are independent of the discovery and validation cohorts; leukemia cells from one patient are sensitive (left) and one resistant to prednisolone (right). Clusters annotated to show CD19+ cells; red denotes control (untreated) and blue depicts cells after treatment with prednisolone 63μM for 96h **(b.)** *CELSR2* expression from clustered single cell populations of sensitive and resistant patients either without treatment or after 96h

prednisolone **(c.)** *BCL2* expression from clustered single cell populations of sensitive and resistant patients **(d.)** Bar plot depicting greater proportion of sensitive leukemia cells (n=2,427 control cells; n= 924 treated cells) killed after treatment with prednisolone for 96h compared to resistant patient (n= 686 control cells; n=759 treated cells; two proportion z-test p-value; **** = $p < 0.0001$). **(e.)** Violin plot representing kernel density of gene expression (individual points represent single cells) of *CELSR2* or **(f.)** *BCL2* in CD19+ leukemia cell populations comparing prednisolone treated to untreated cells in sensitive (n=2,427 control cells; n= 924 treated cells) or resistant patients (n= 686 control cells; n=759 treated cells; ** = $p < 0.01$).

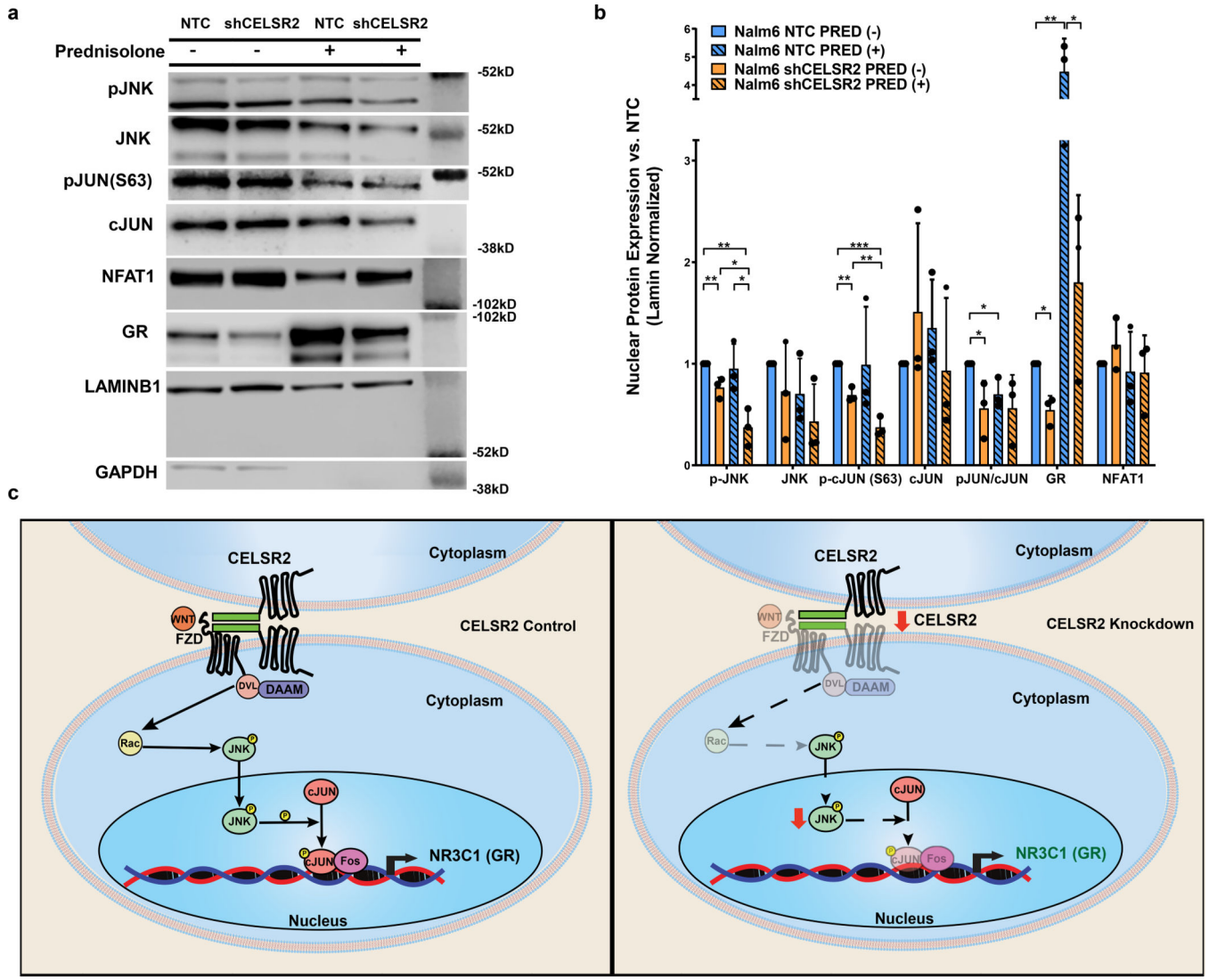

Figure 8. Perturbation of downstream non-canonical Wnt signaling leads to decreased GR expression and glucocorticoid resistance.

(a.) Representative western blot and **(b.)** Barplot (n= 3 independent experiments; mean ± S.D.) depicting nuclear protein expression of signaling components from the planar cell polarity and Ca^{2+}/NFAT non-canonical Wnt signaling pathway, *CELSR2* knockdown (shCELSR2) vs. non-target control cells (NTC) with or without 10μM prednisolone treatment for 24hr (two-tailed t-test p-values; * P < 0.05; ** P< 0.01***; P <0.001; **** P<0.0001). **(c.)** Schematic representation of non-canonical Wnt signaling, depicting proposed mechanism by which low *CELSR2* expression leads to decreased expression of the GR (right panel).